Supplement of Atmos. Chem. Phys., 17, 3145–3163, 2017
http://www.atmos-chem-phys.net/17/3145/2017/
doi:10.5194/acp-17-3145-2017-supplement


Atmospheric Chemistry and Physics Open Access EGU

*Supplement of*

# The contribution of wood burning and other pollution sources to wintertime organic aerosol levels in two Greek cities

**Kalliopi Florou et al.**

*Correspondence to:* Spyros N. Pandis (spyros@chemeng.upatras.gr)

# 1. Location of sampling sites


**Figure S1.** The location of the sampling sites: (a) the cities of Patras and Athens in Greece; (b) the National Observatory (Thiseio) in Athens; and (c) the Technological Educational Institute (TEI) and the city center of Patras.

## 2. Origin of air masses in Patras

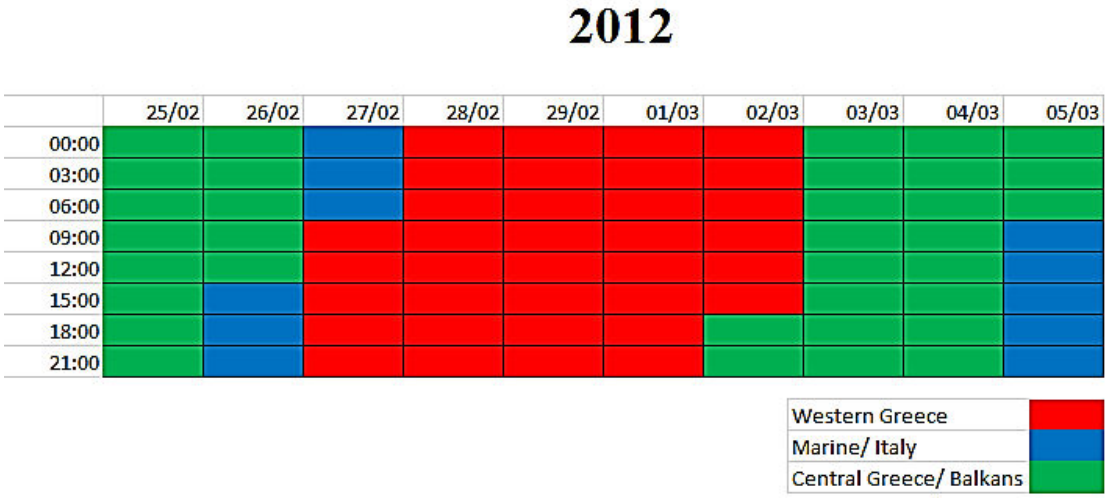


**Figure S2.** FLEXPART analysis for the Patras campaign. The origin of the air mass every 3 h for all the sampling days is shown.

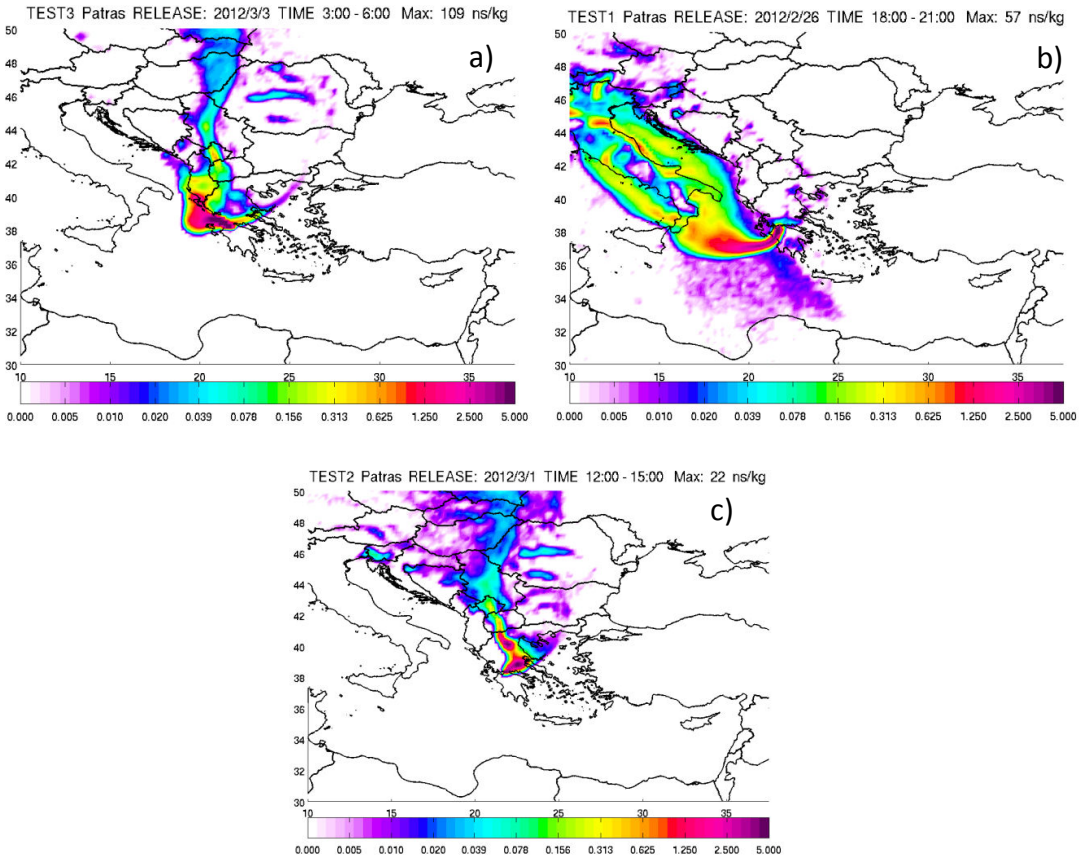


**Figure S3.** Examples of the three categories of back-trajectories of air masses arriving in Patras: a) western Greece; b) marine/Italy; and c) central Greece/Balkans.

## 3. Origin of air masses in Athens

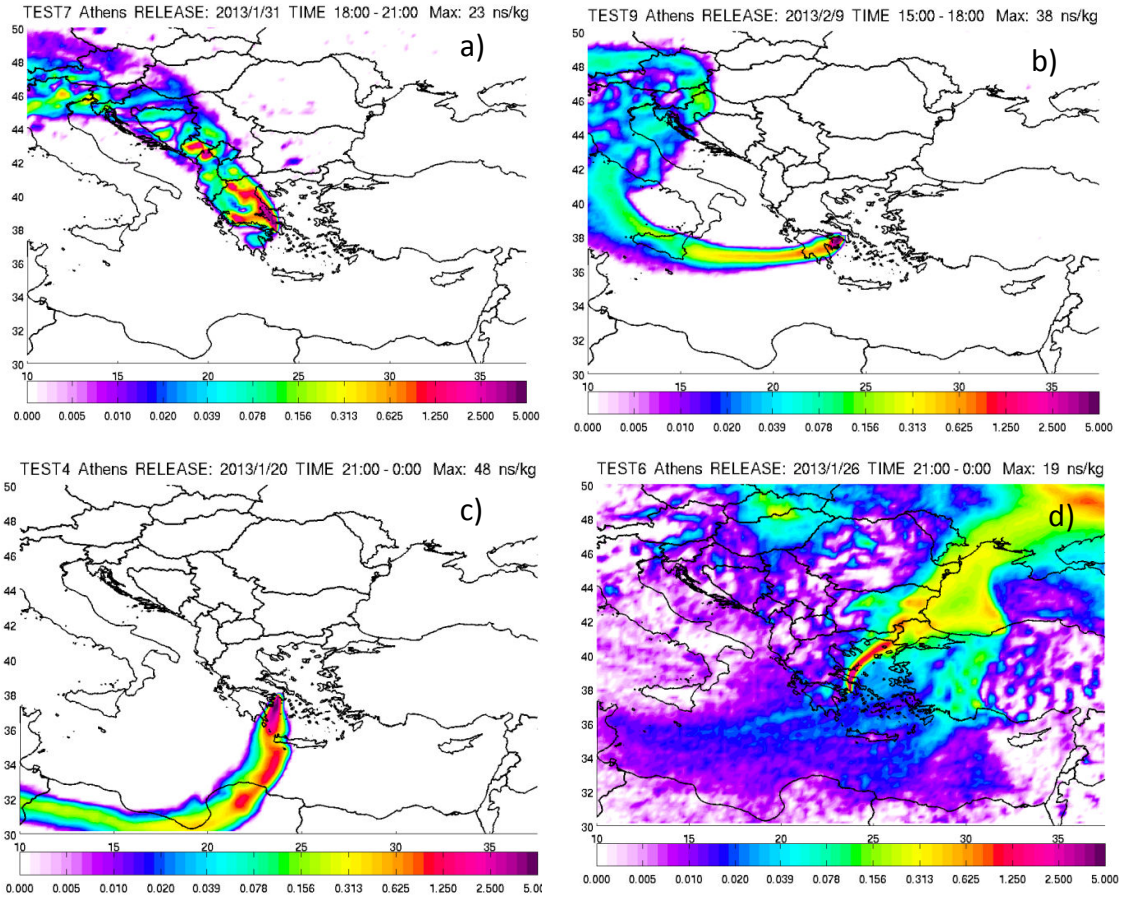


**Figure S4.** Examples of the three categories of back-trajectories of air masses arriving in Athens: (a) Greece-Balkans; (b) marine (Sicily); (c) Africa and (d) Aegean/NE.

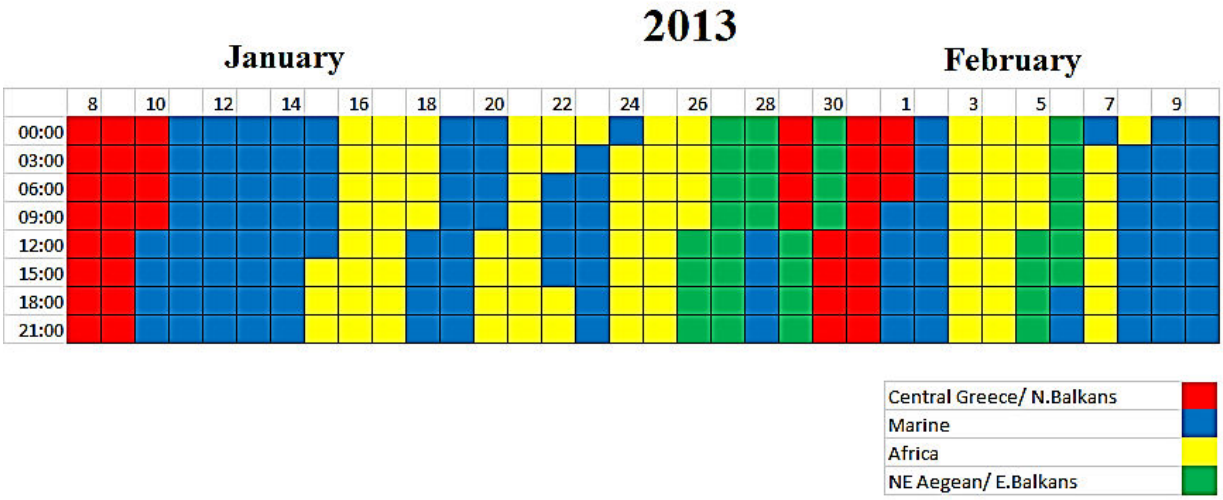


**Figure S5.** FLEXPART analysis for the Athens campaign. The origin of the air mass every 3 h for all the sampling days is shown.

## 4. Rain events in Athens

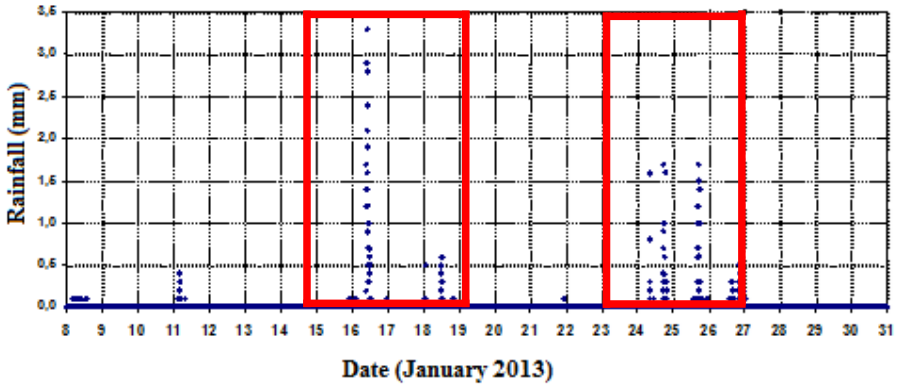


**Figure S6.** Cumulative precipitation at 5-min intervals in the center of Athens during January 2013. The red boxes show the two periods with frequent precipitation.

## 5. Average AMS size distributions

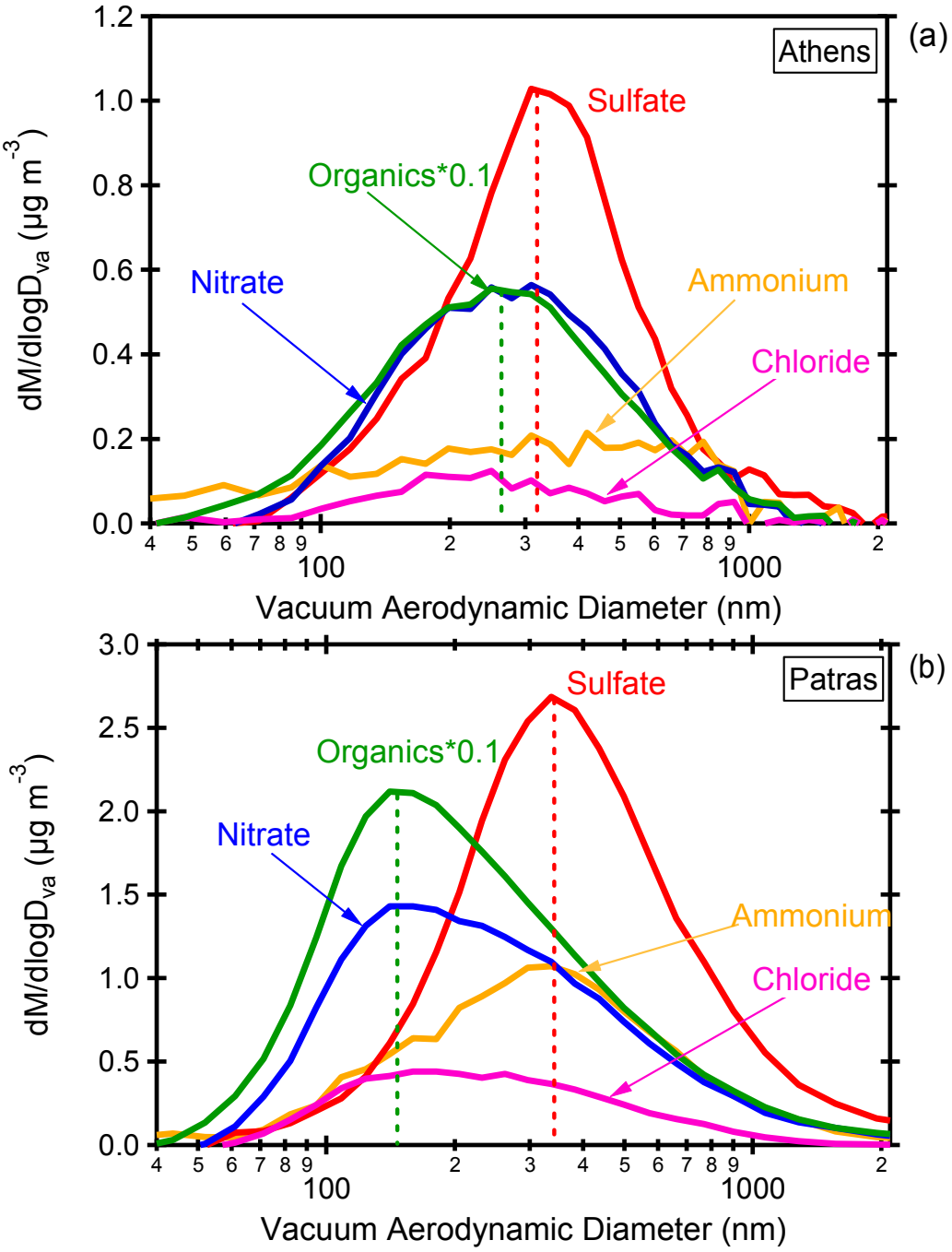


**Figure S7.** The average HR-AMS size distributions as a function of vacuum aerodynamic diameter for: (a) Athens and (b) Patras. The mean mode of the size distribution of the organics (140 nm) and sulfate (330 nm) are marked with dashed lines (green and red, respectively).

## 6. Elemental ratios and carbon oxidation state ($OS_C$)

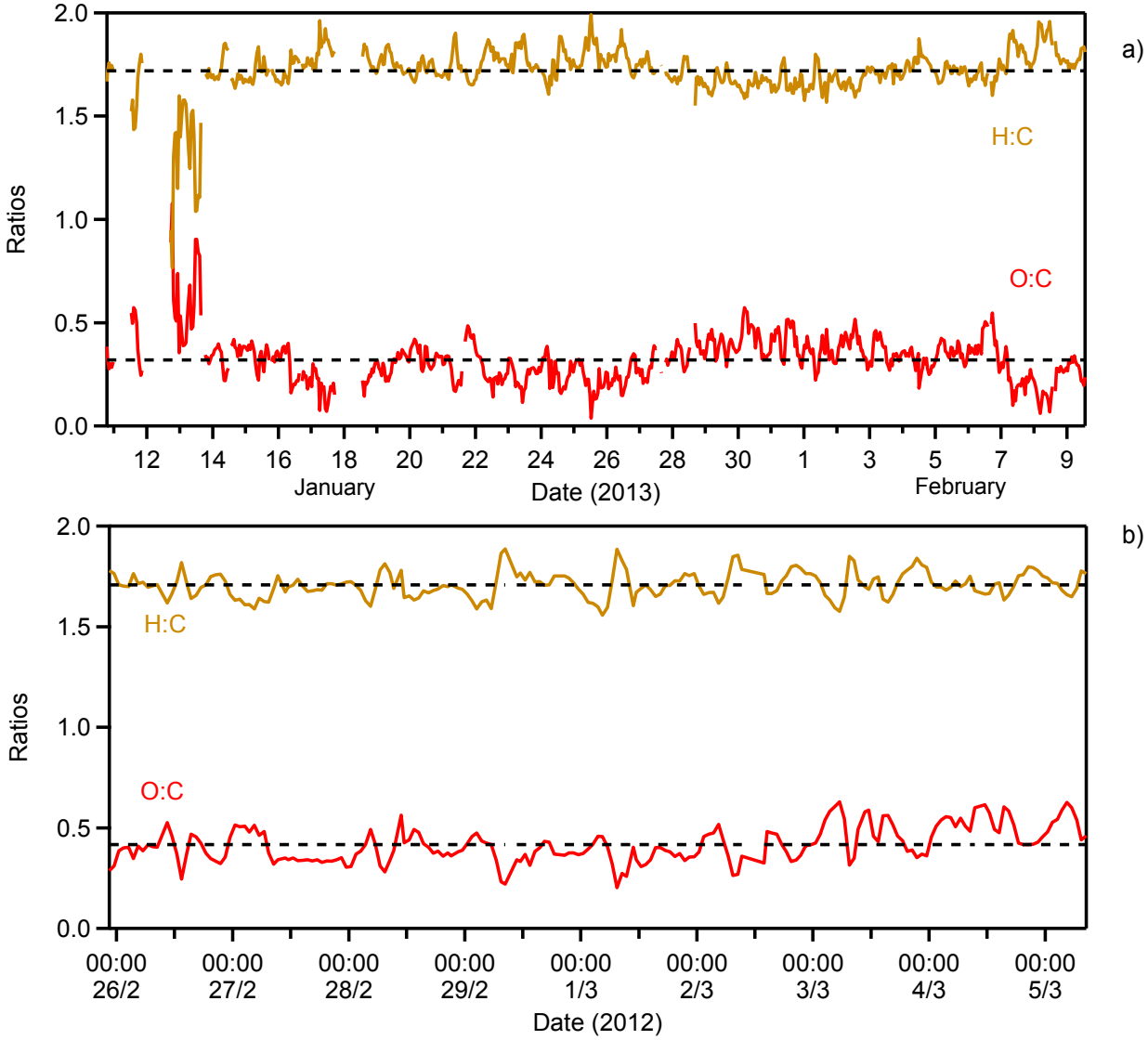


**Figure S8.** Time series of the OA O:C and H:C ratios for: a) Athens and b) Patras based on the approach of Canagaratna et al. (2015). Their mean values are shown with dashed lines.

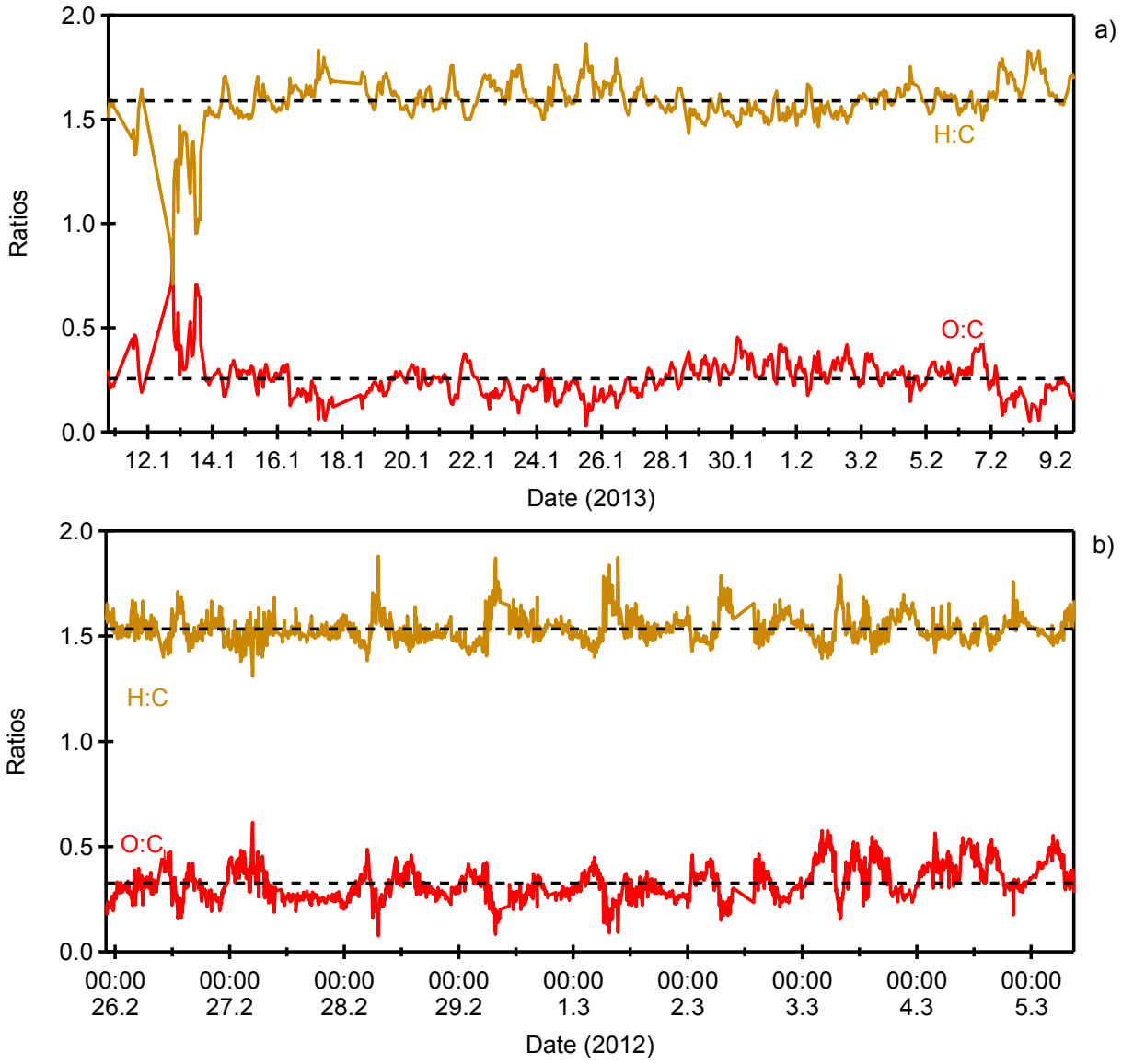


**Figure S9.** O:C and H:C elemental ratios in: a) Athens and b) Patras based on the approach of Aiken et al. (2008). Their mean value is shown with dashed lines.

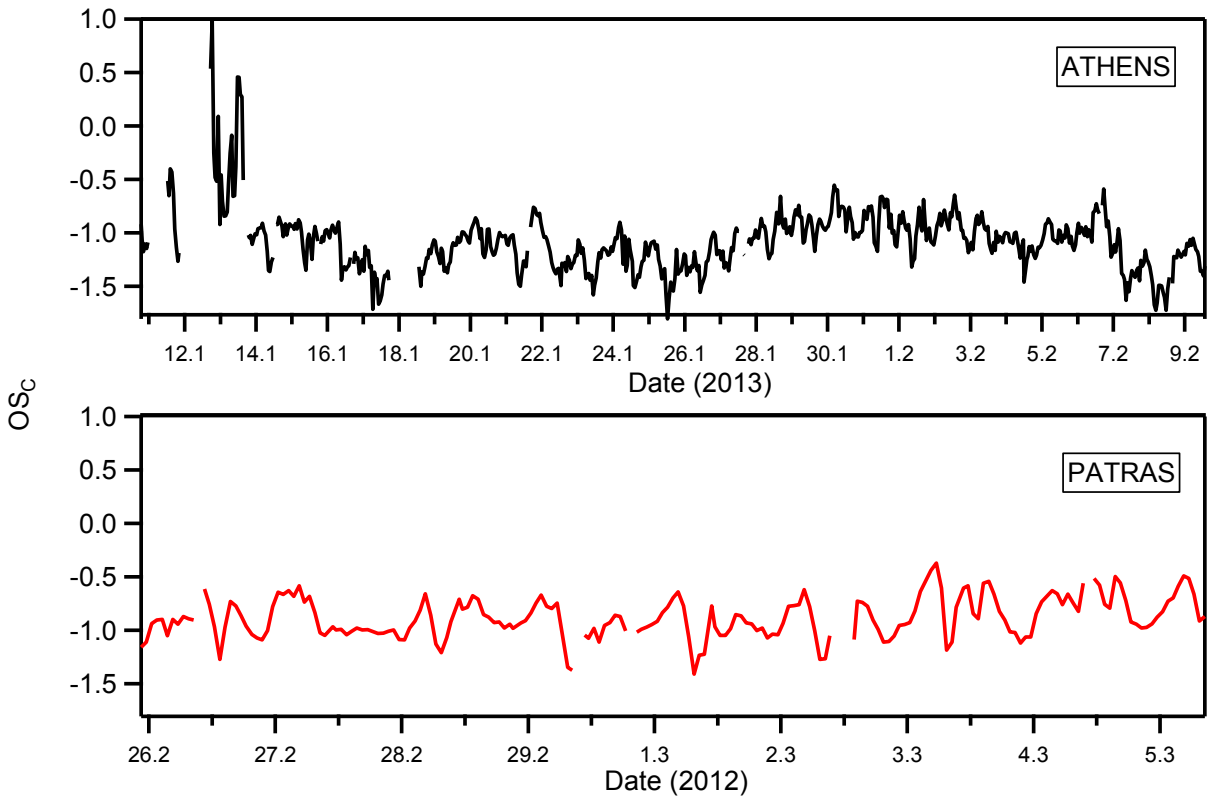


**Figure S10.** Average carbon oxidation state $OS_C$ for the two cities.

## 7a. PMF solution choice for Patras

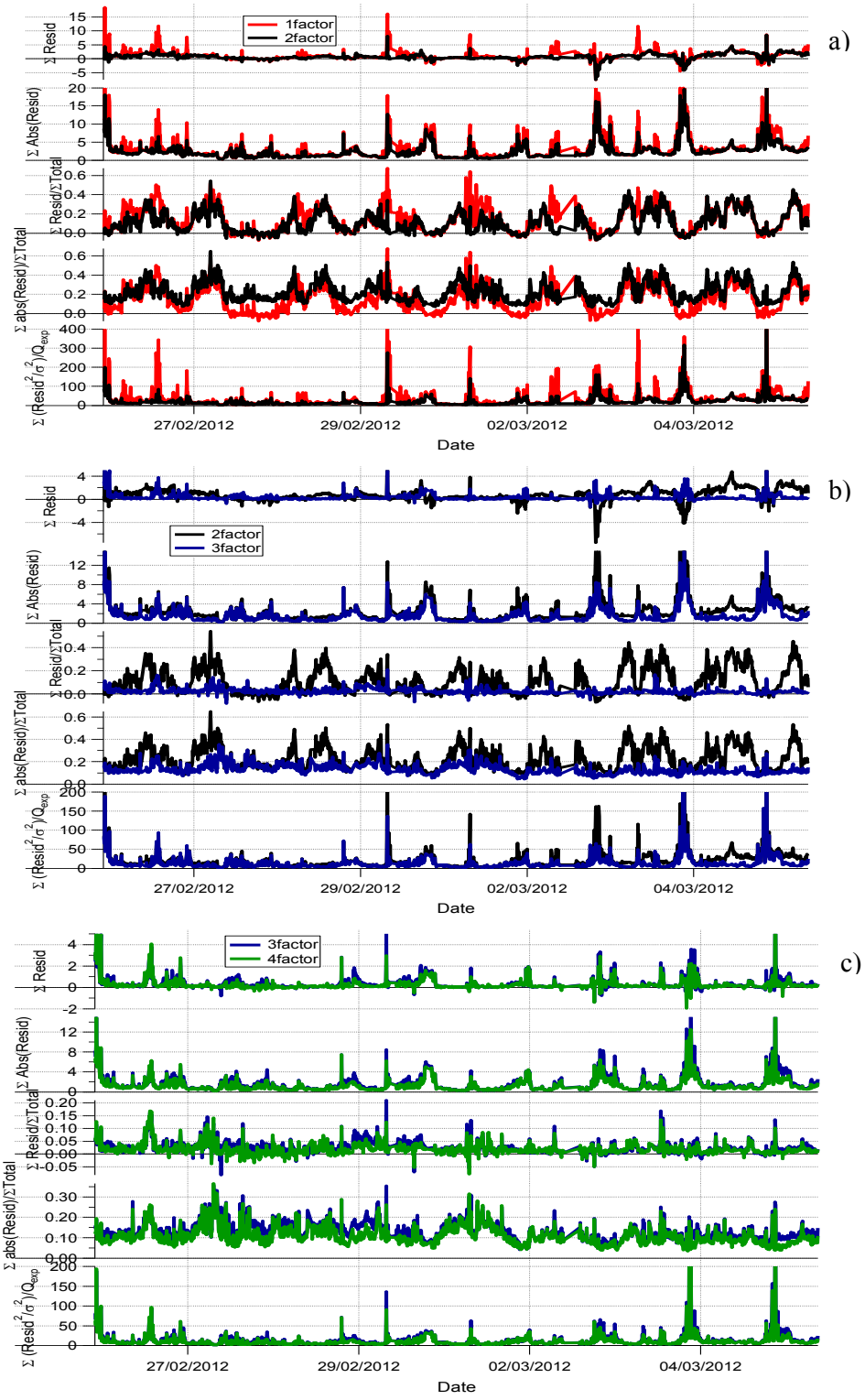


**Figure S11**. Model residuals **E= X-GF** calculated using the PMF evaluation tool PET (Ulbrich et al., 2009) for Patras. Comparison between (a) 1-factor (red lines) and 2-factor (black lines) PMF solutions, (b) 2-factor (black lines) and 3-factor (blue lines) PMF solutions, and (c) 3-factor (blue lines) and 4-factor (green lines) PMF solutions.

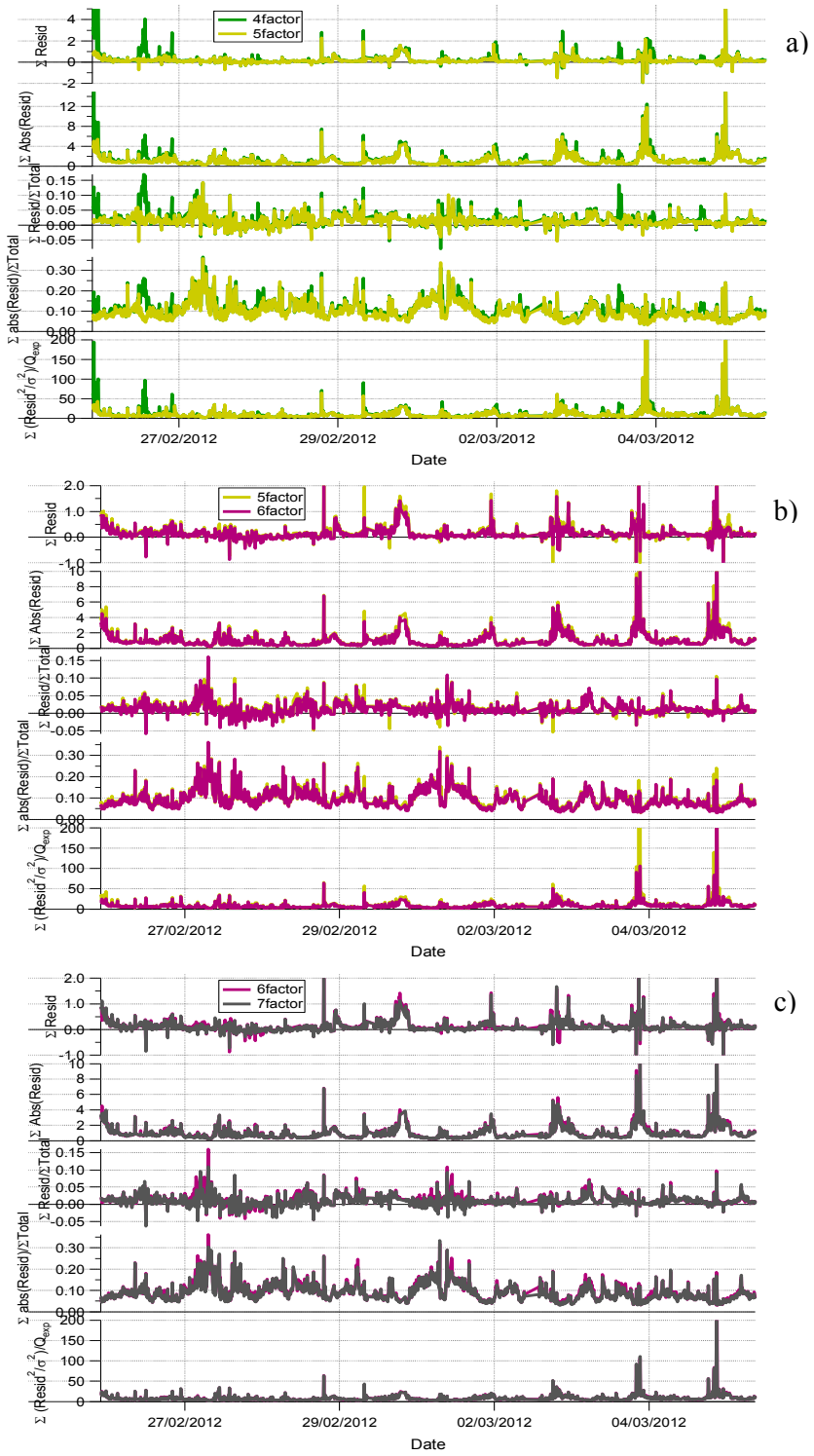


**Figure S12**. Model residuals **E=X-GF** calculated using the PMF evaluation tool PET (Ulbrich et al., 2009) for Patras. Comparison between a) 4-factor (green lines) and 5-factor (yellow lines) solutions, (b) 5-factors (yellow lines) and 6-factors (pink lines), and (c) 6-factors (pink lines) and 7-factors (grey lines) PMF solutions. The residuals decreased from 4 to 5 factors especially for the first days of the campaign and March 4. The 5, 6 and 7 factor solution residuals were almost identical.

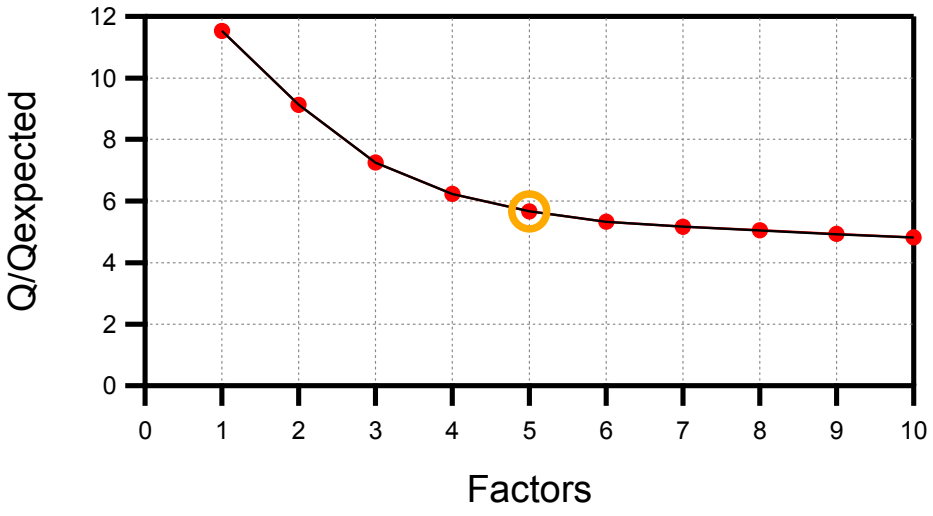


**Figure S13.** $Q/Q_{expected}$ vs. the number of the factors in Patras.

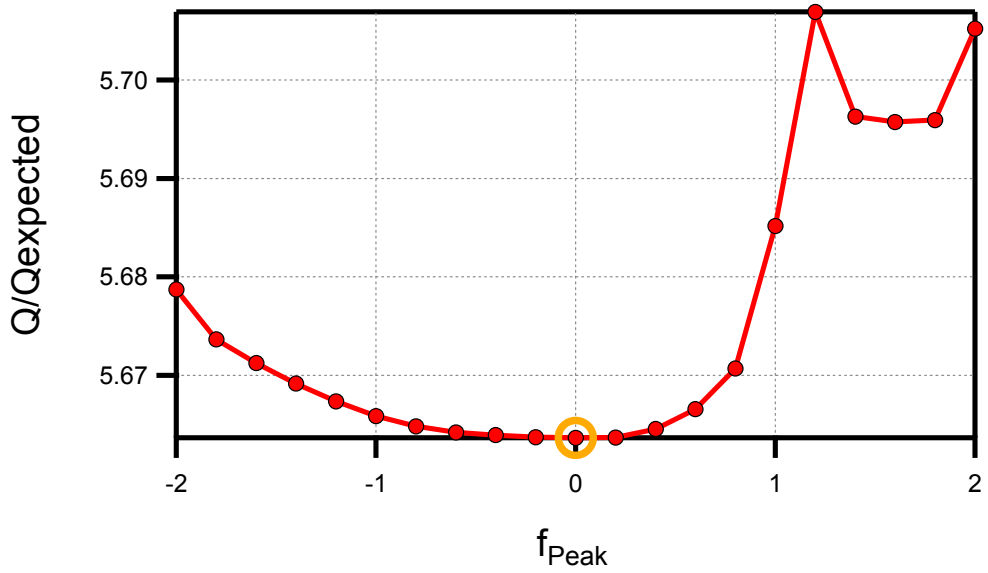


**Figure S14.** $Q/Q_{expected}$ for $f_{peak}$ -2 to 2 for the 5-factor solution in Patras. There is a stable area between $f_{peak}$ -0.6 and 0.2, with the lower $Q/Q_{expected}$ at $f_{peak}$=0.0 and $f_{peak}$=0.2.

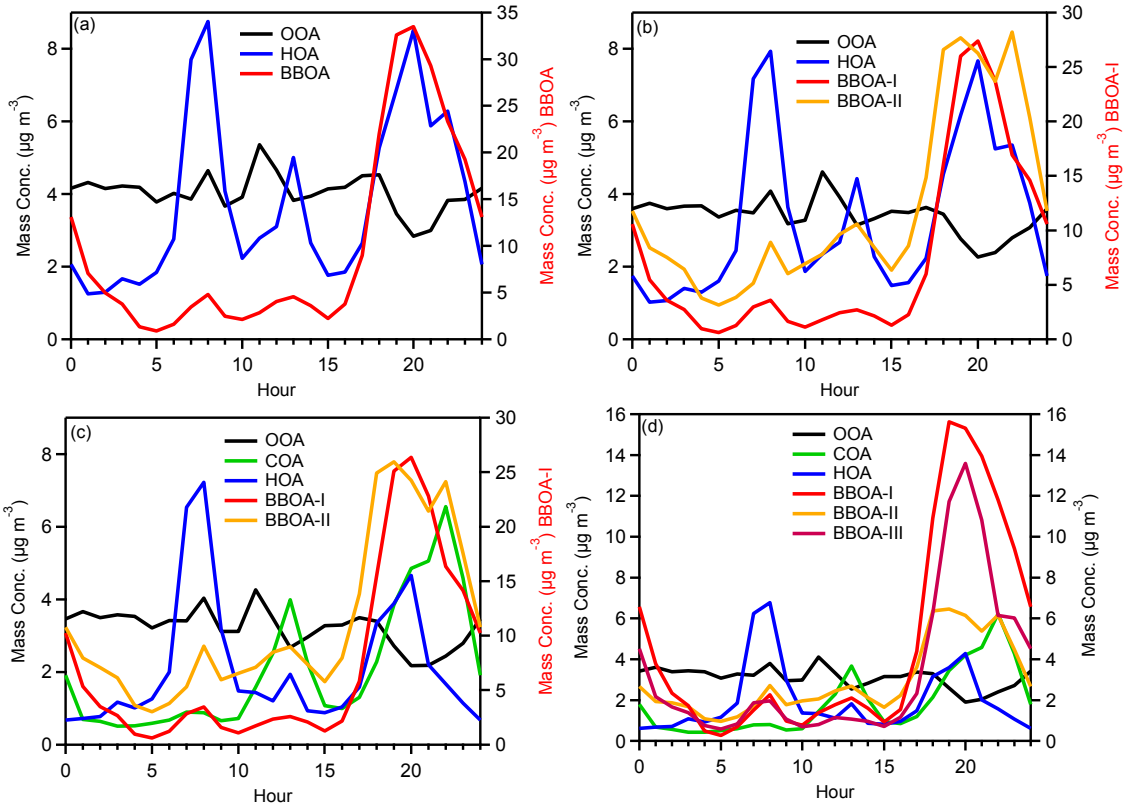


**Figure S15.** Average diurnal profiles of the mass concentration for the: (a) 3, (b) 4, (c) 5 and (d) 6 factor PMF solutions in Patras.

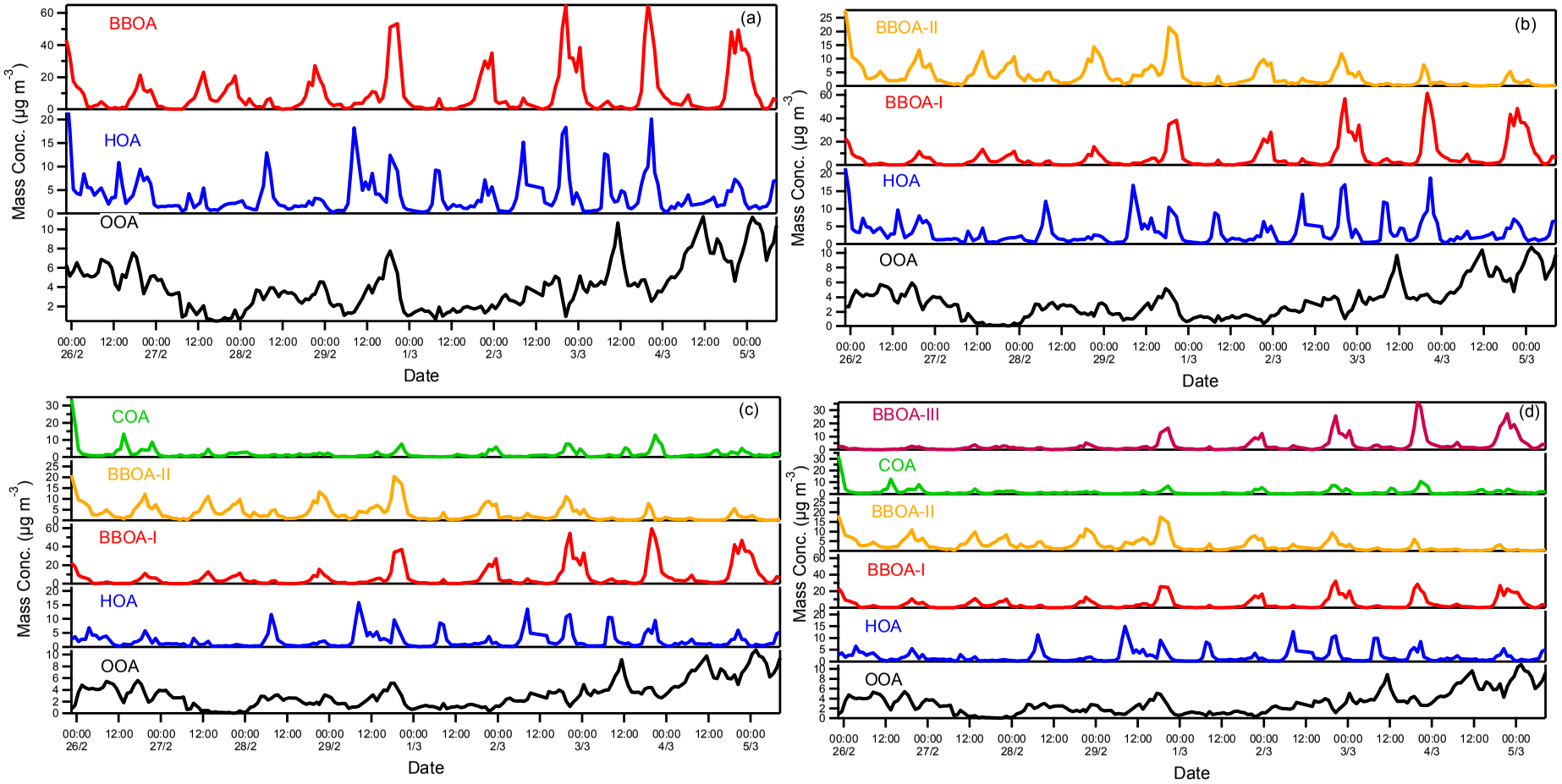


**Figure S16.** Time series for the: (a) 3, (b) 4, (c) 5 and (d) 6 factor PMF solutions in Patras.

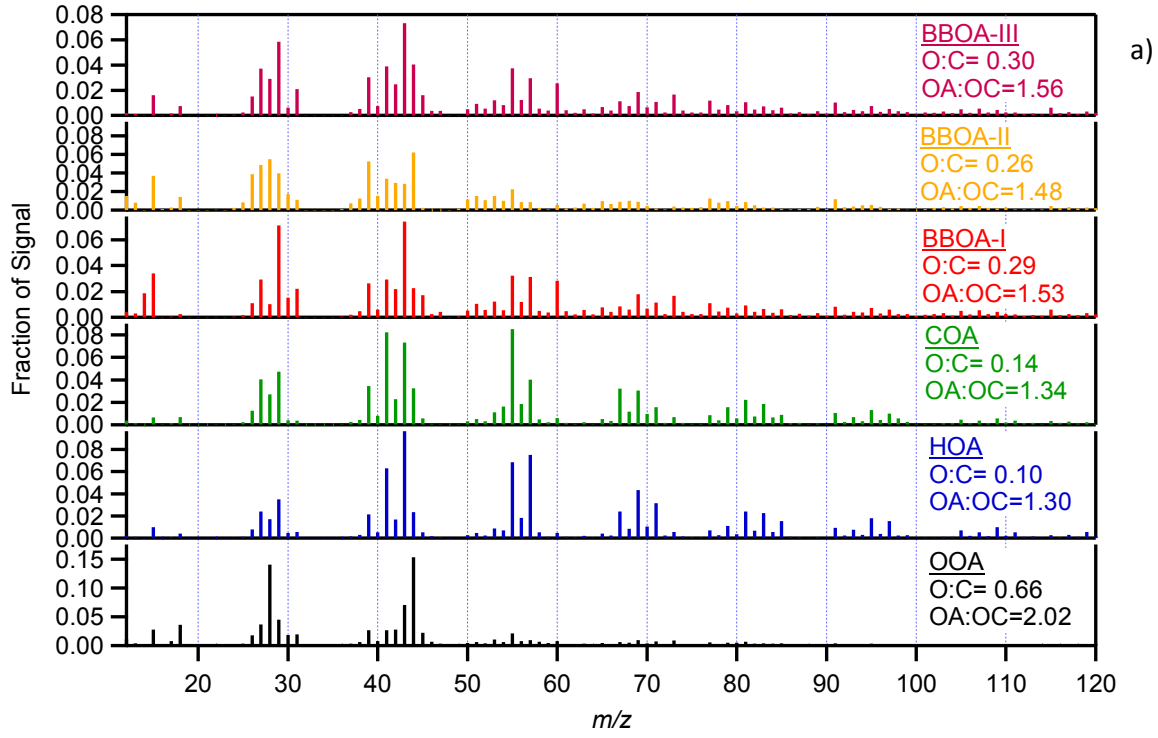
a)
Fraction of Signal
BBOA-III
O:C= 0.30
OA:OC=1.56
BBOA-II
O:C= 0.26
OA:OC=1.48
BBOA-I
O:C= 0.29
OA:OC=1.53
COA
O:C= 0.14
OA:OC=1.34
HOA
O:C= 0.10
OA:OC=1.30
OOA
O:C= 0.66
OA:OC=2.02
m/z

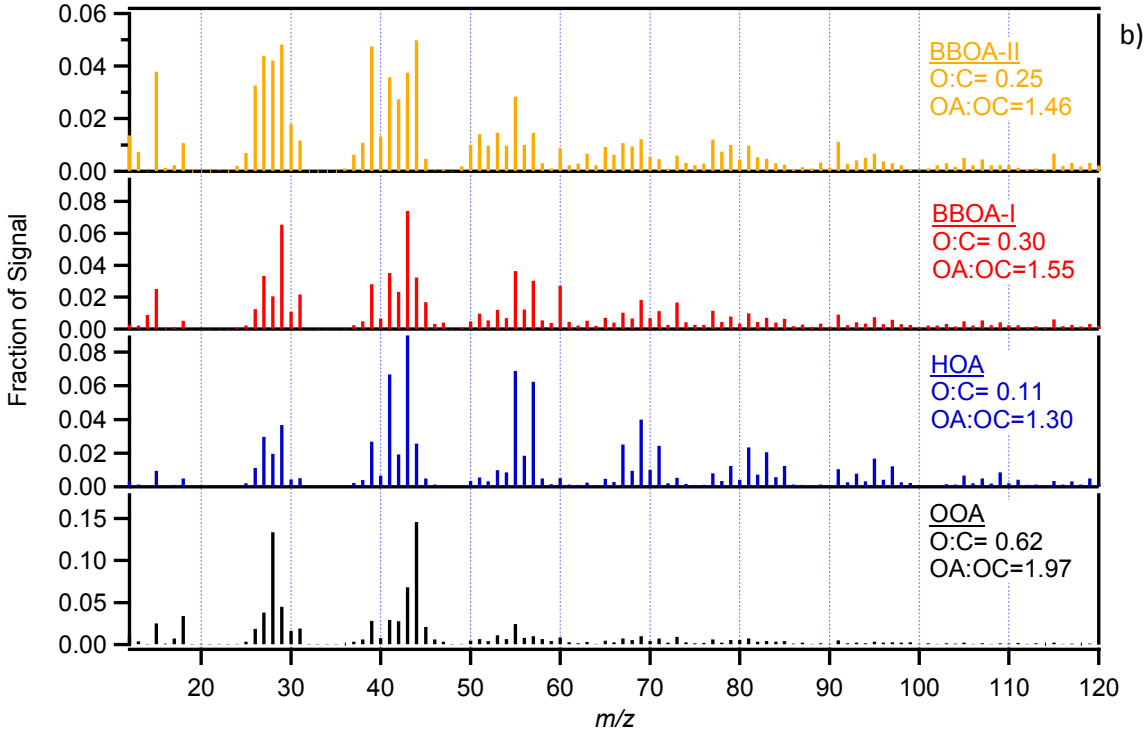
b)
Fraction of Signal
BBOA-II
O:C= 0.25
OA:OC=1.46
BBOA-I
O:C= 0.30
OA:OC=1.55
HOA
O:C= 0.11
OA:OC=1.30
OOA
O:C= 0.62
OA:OC=1.97
m/z

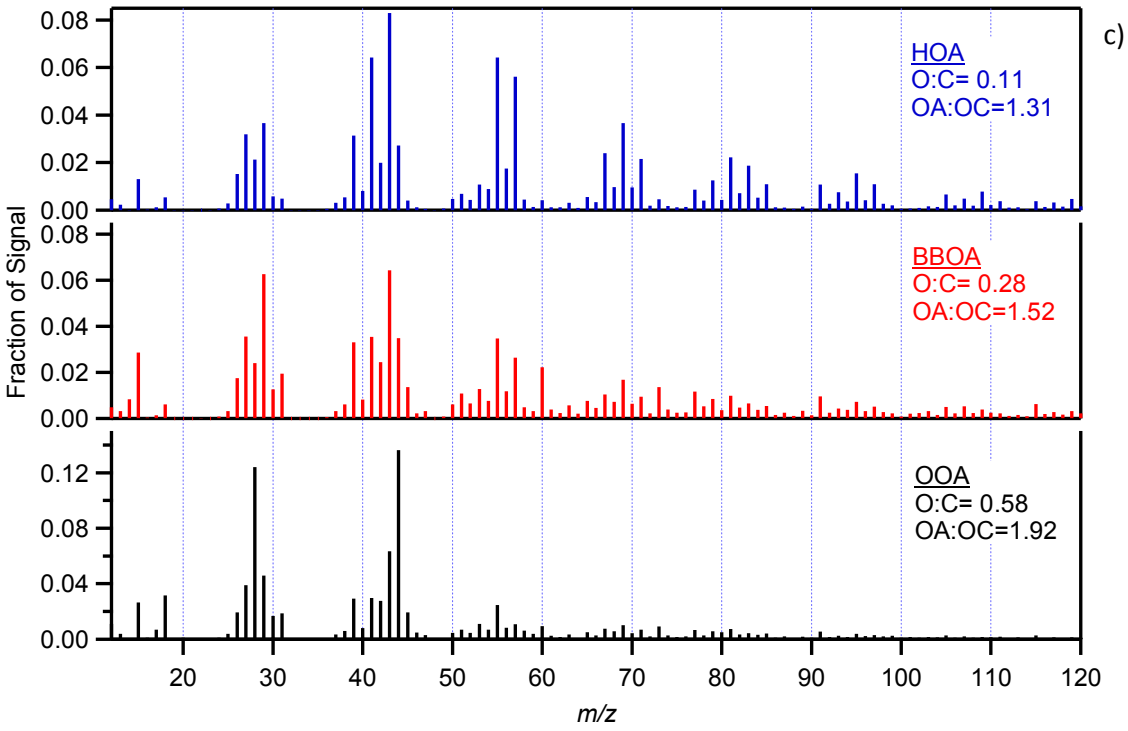


**Figure S17.** AMS spectra for the (a) 6, (b) 4 and (c) 3-factor PMF solutions in Patras.

## 7b. PMF solution choice for Athens

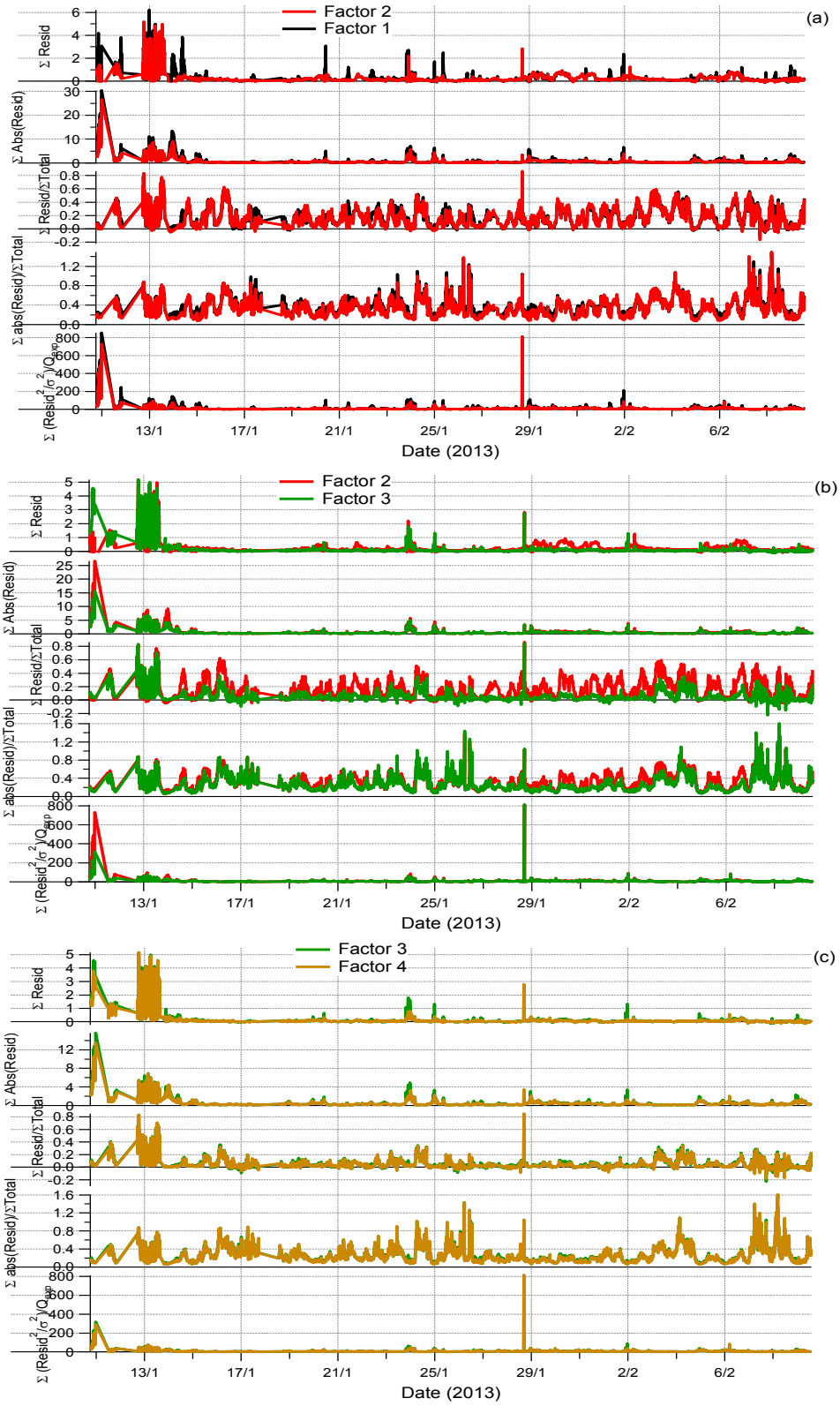


**Figure S18**. Model residuals **E= X-GF** calculated using the PMF evaluation tool, PET (Ulbrich et al., 2009) for Athens. Comparison between (a) 1-factor (black lines) and 2-factor (red lines) PMF solutions, (b) 2-factor (red lines) and 3-factor (green lines) PMF solutions, and (c) 3-factor (green lines) and 4-factor (yellow lines) PMF solutions.

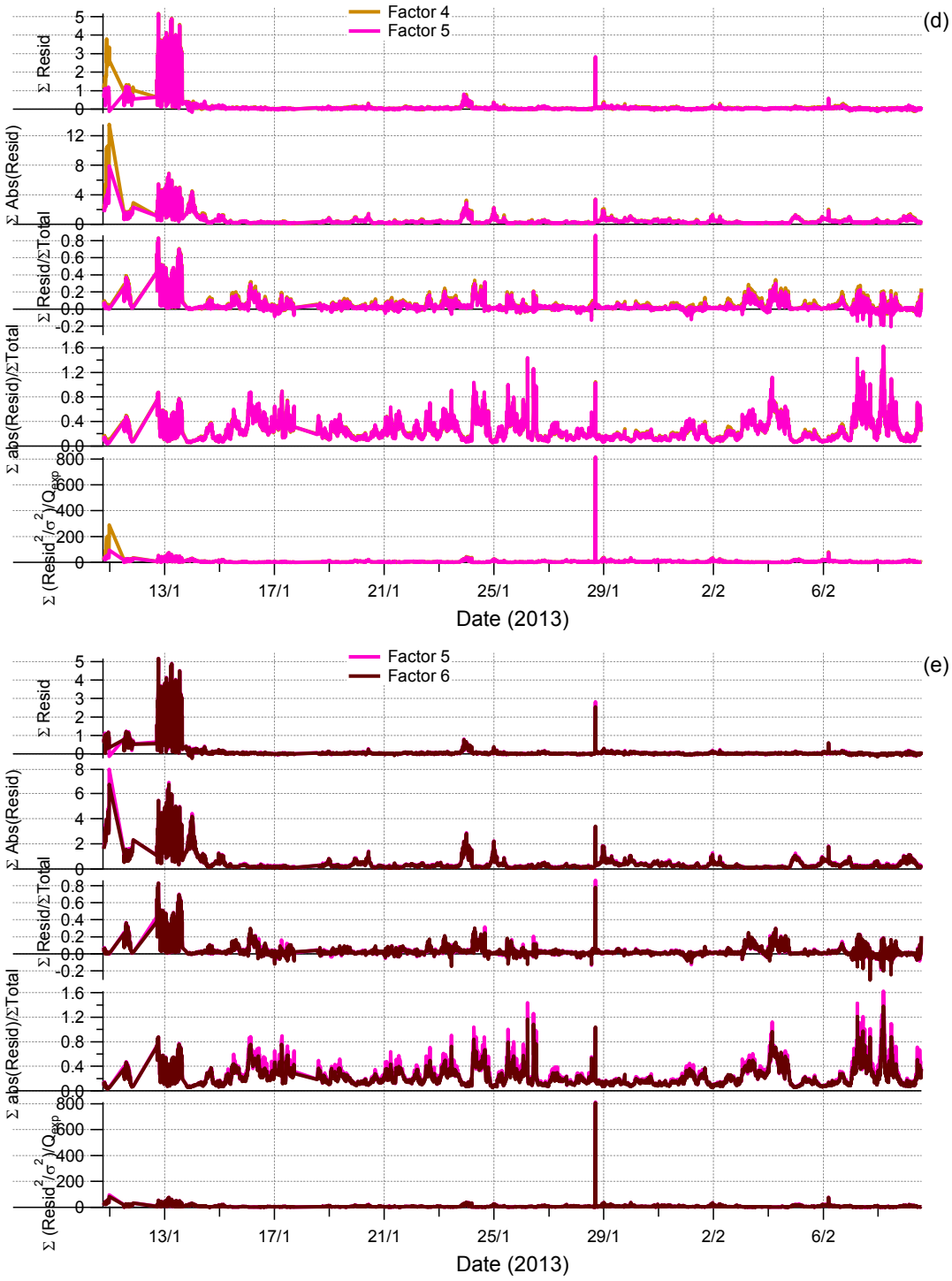


**Figure S19**. Model residuals **E=X-GF** calculated using the PMF evaluation tool, PET (Ulbrich et al., 2009) for Athens. Comparison between (d) 4-factor (yellow lines) and 5-factor (pink lines) solutions, and (e) 5-factor (pink lines) and 6-factor (brown lines) PMF solutions.

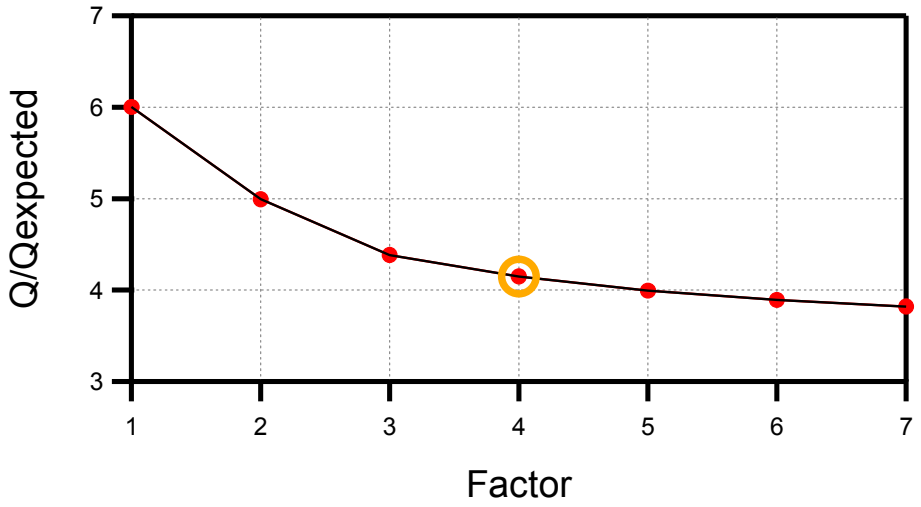


**Figure S20.** $Q/Q_{expected}$ vs. the number of the factors for Athens.

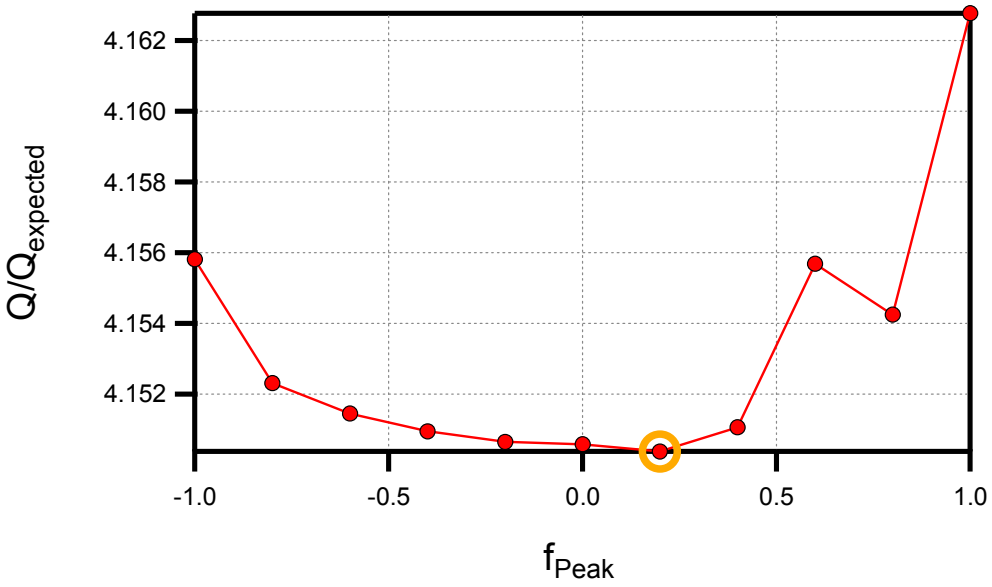


**Figure S21.** $Q/Q_{expected}$ for $f_{peak}$ -1 to 1 for a 4 factor solution for Athens. There is a stable area between the $f_{peak}$ -0.4 and 0.2, with the lower $Q/Q_{expected}$ at $f_{peak}$=0.2.

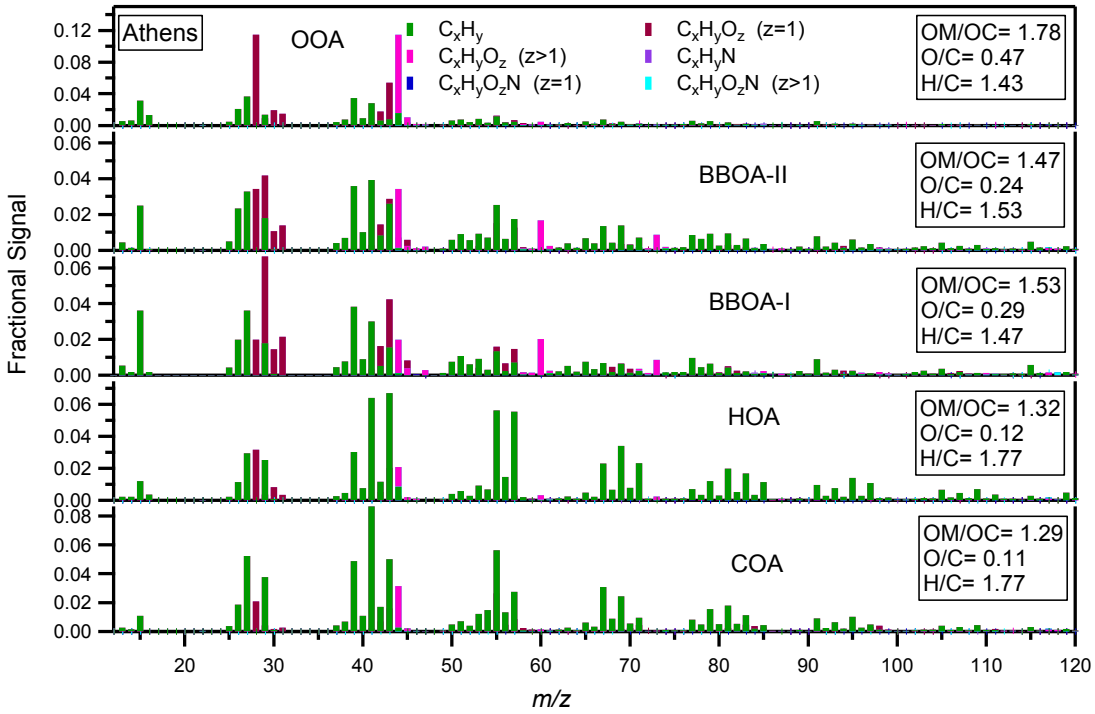


**Figure S22.** High resolution spectra by the AMS for the 5-factor PMF solution for Athens.

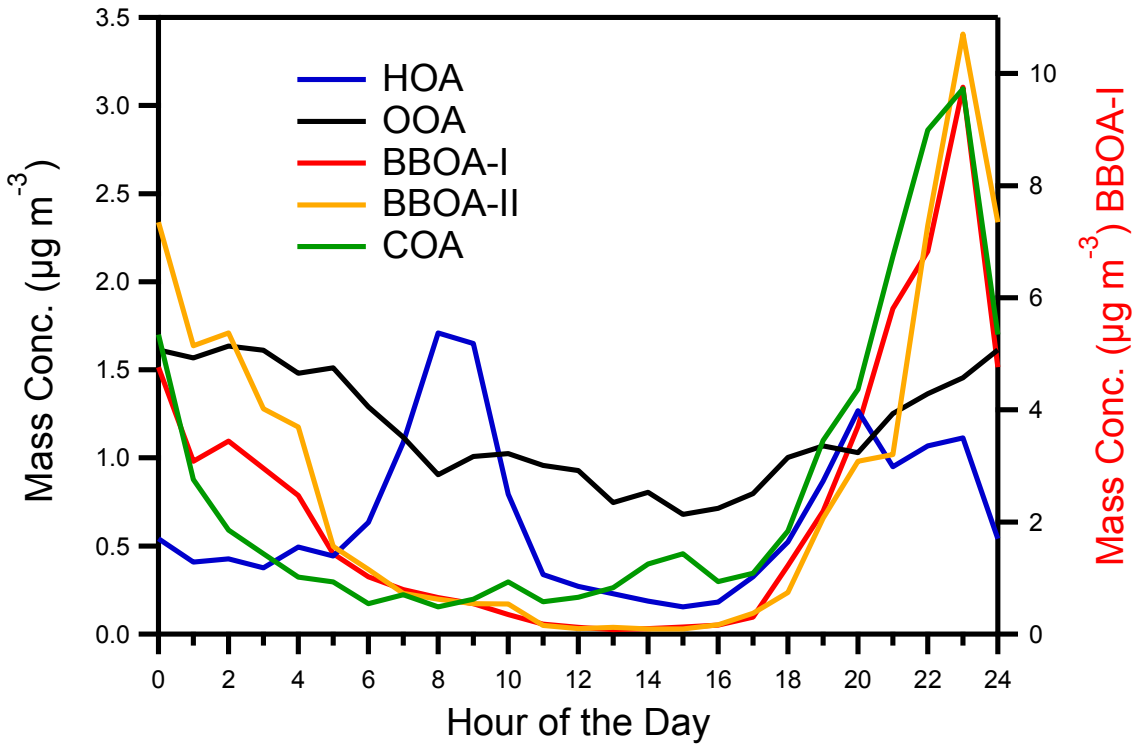


**Figure S23.** Diurnal profiles of the mass concentration for the 5 factor PMF solution in Athens. The BBOA-I mass concentration appears on the right y-axis.

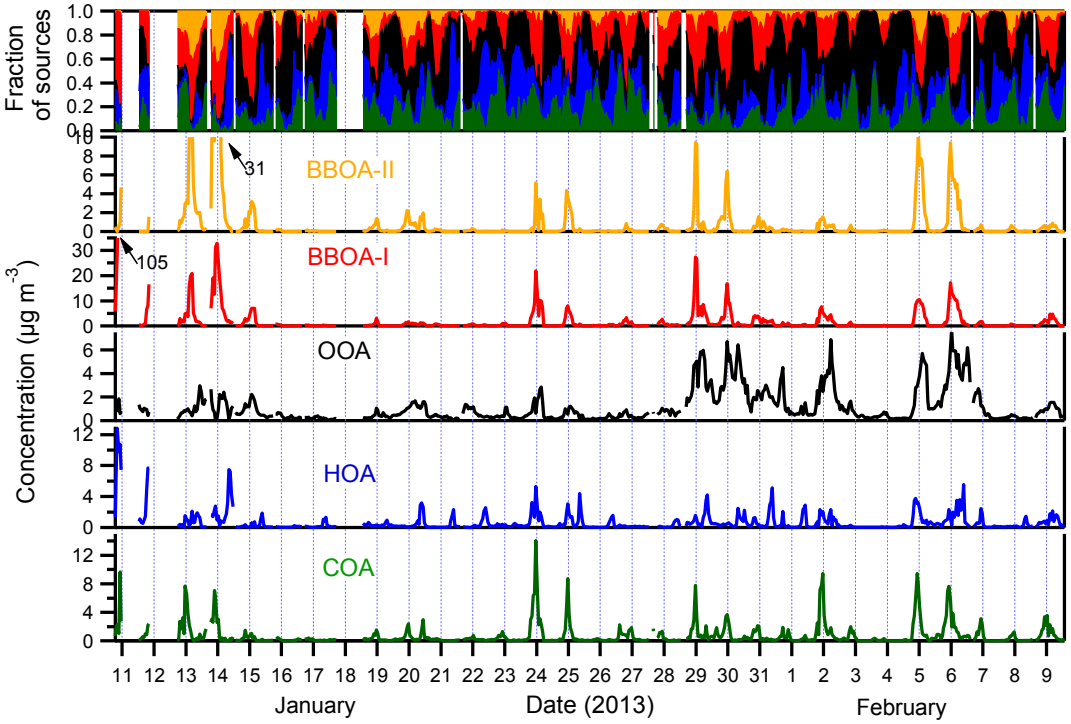


**Figure S24.** Time series of the 5-factor solution for Athens. The $PM_1$ OA composition is also shown. During the first day, BBOA-I reached levels up to 105 μg $m^{-3}$ and during the 15th of January, BBOA-II was equal to 31 μg $m^{-3}$.

**Table S1.** Correlation between the 5 factors in Athens and VOCs as measured by the PTR-MS.

| $R^2$ | BBOA-II | BBOA-I | HOA | COA | OOA |
|---|---|---|---|---|---|
| m/z 42 (Acetonitrile) | 0.43 | 0.74 | 0.57 | 0.32 | 0.10 |
| m/z 43 | 0.43 | 0.63 | 0.53 | 0.28 | 0.09 |
| m/z 47 (formic acid) | 0.26 | 0.39 | 0.50 | 0.10 | 0.02 |
| m/z 59 (acetone, glyoxal) | 0.39 | 0.64 | 0.57 | 0.28 | 0.15 |
| m/z 61 (acetic acid) | 0.39 | 0.41 | 0.27 | 0.16 | 0.07 |
| m/z 69 (isoprene, furan) | 0.50 | 0.79 | 0.42 | 0.28 | 0.06 |
| m/z 71 (MVK, MACR) | 0.40 | 0.78 | 0.59 | 0.29 | 0.06 |
| m/z 73 (MEK) | 0.42 | 0.68 | 0.51 | 0.28 | 0.12 |
| m/z 75 (hydroxyacetone) | 0.41 | 0.60 | 0.22 | 0.21 | 0.03 |
| m/z 79 (benzene) | 0.34 | 0.68 | 0.65 | 0.28 | 0.08 |
| m/z 81 (terpenes) | 0.51 | 0.75 | 0.46 | 0.27 | 0.06 |
| m/z 85 (EVK) | 0.49 | 0.83 | 0.46 | 0.31 | 0.06 |
| m/z 87 (MBO, C5, methacrylic acid) | 0.55 | 0.83 | 0.33 | 0.30 | 0.07 |
| m/z 93 (toluene) | 0.15 | 0.39 | 0.66 | 0.17 | 0.05 |
| m/z 95 (2 vinyl furan, phenol) | 0.22 | 0.42 | 0.21 | 0.11 | 0.00 |
| m/z 99 (hexenal) | 0.52 | 0.76 | 0.39 | 0.31 | 0.10 |
| m/z 101 (isoprene hyperoxides) | 0.39 | 0.64 | 0.28 | 0.22 | 0.06 |
| m/z 105(styrene) | 0.25 | 0.53 | 0.48 | 0.17 | 0.05 |
| m/z 107 (xylenes) | 0.19 | 0.48 | 0.77 | 0.21 | 0.06 |
| m/z 113 (chlorobenzene) | 0.51 | 0.69 | 0.37 | 0.28 | 0.11 |
| m/z 115 (heptanal) | 0.38 | 0.60 | 0.32 | 0.20 | 0.06 |
| m/z 121 (C9 aromatics) | 0.20 | 0.48 | 0.76 | 0.20 | 0.06 |
| m/z 129 (octanal, naphthalene) | 0.30 | 0.72 | 0.51 | 0.19 | 0.04 |
| m/z 135 (C10 aromatics) | 0.23 | 0.50 | 0.71 | 0.20 | 0.07 |
| m/z 137 (monoterpenes) | 0.48 | 0.60 | 0.45 | 0.23 | 0.09 |
| m/z 139 (nopinone) | 0.50 | 0.54 | 0.31 | 0.20 | 0.08 |
| m/z 151 (pinonaldehyde) | 0.21 | 0.28 | 0.21 | 0.08 | 0.02 |
| m/z 163 (C12 aromatics) | 0.33 | 0.28 | 0.29 | 0.09 | 0.05 |

## 7. Comparison of BBOA and $K^+$ in Athens

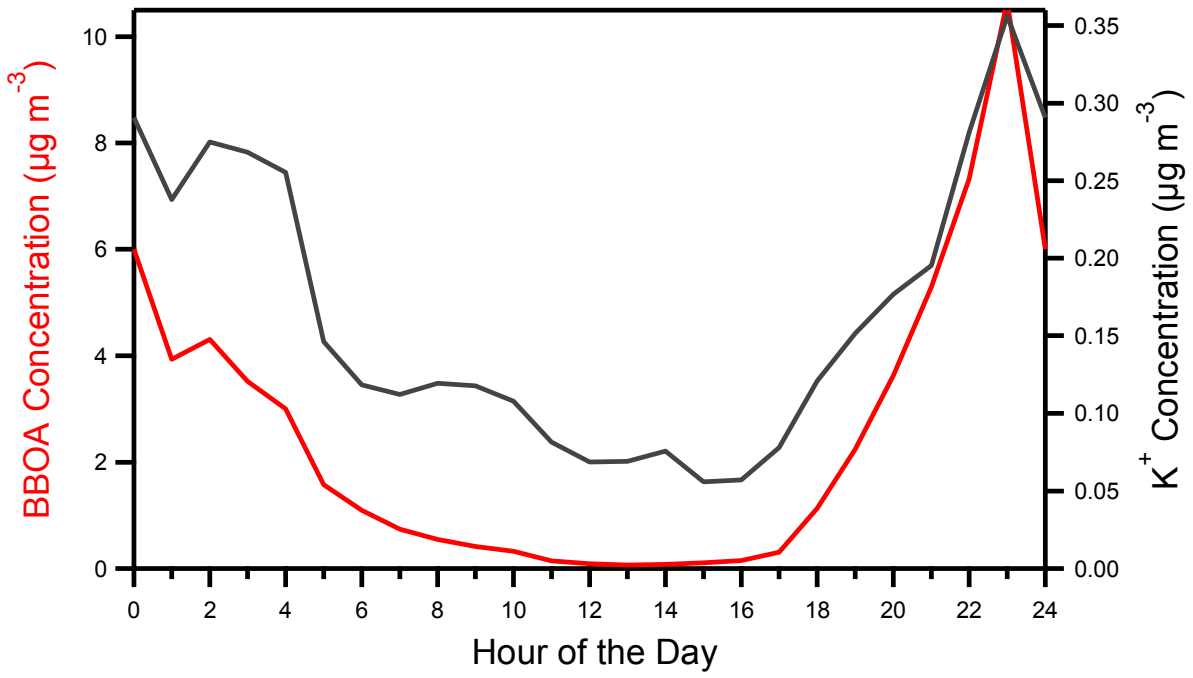


**Figure S25.** The diurnal profiles of the BBOA (red) and $K^+$ (grey) in Athens.

## 8. Comparison of the PMF factors' spectra for the two cities

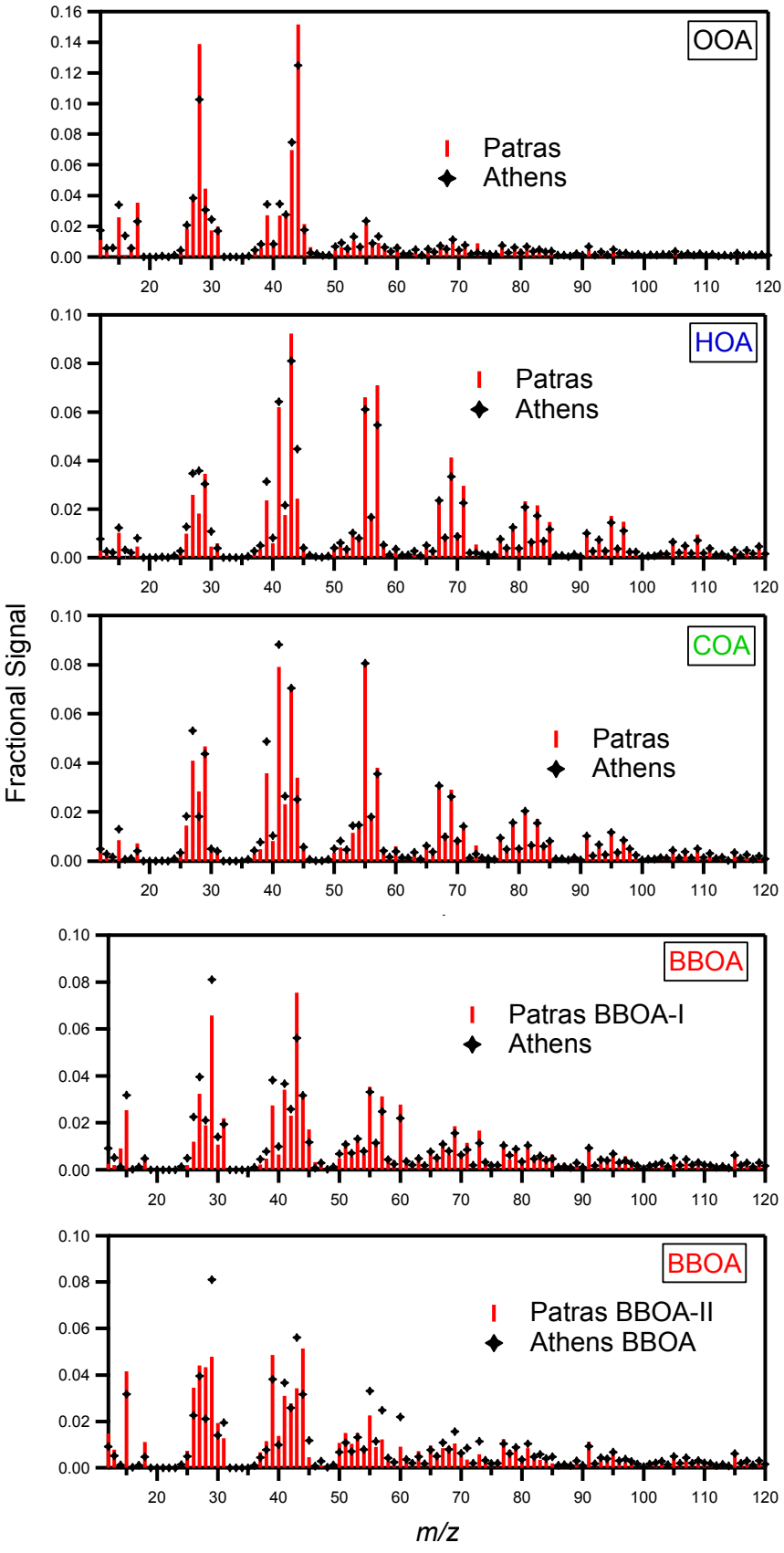


**Figure S26.** Comparison of the PMF-factor mass spectra for the two cities.

## 9. Comparison of factor spectra with other studies

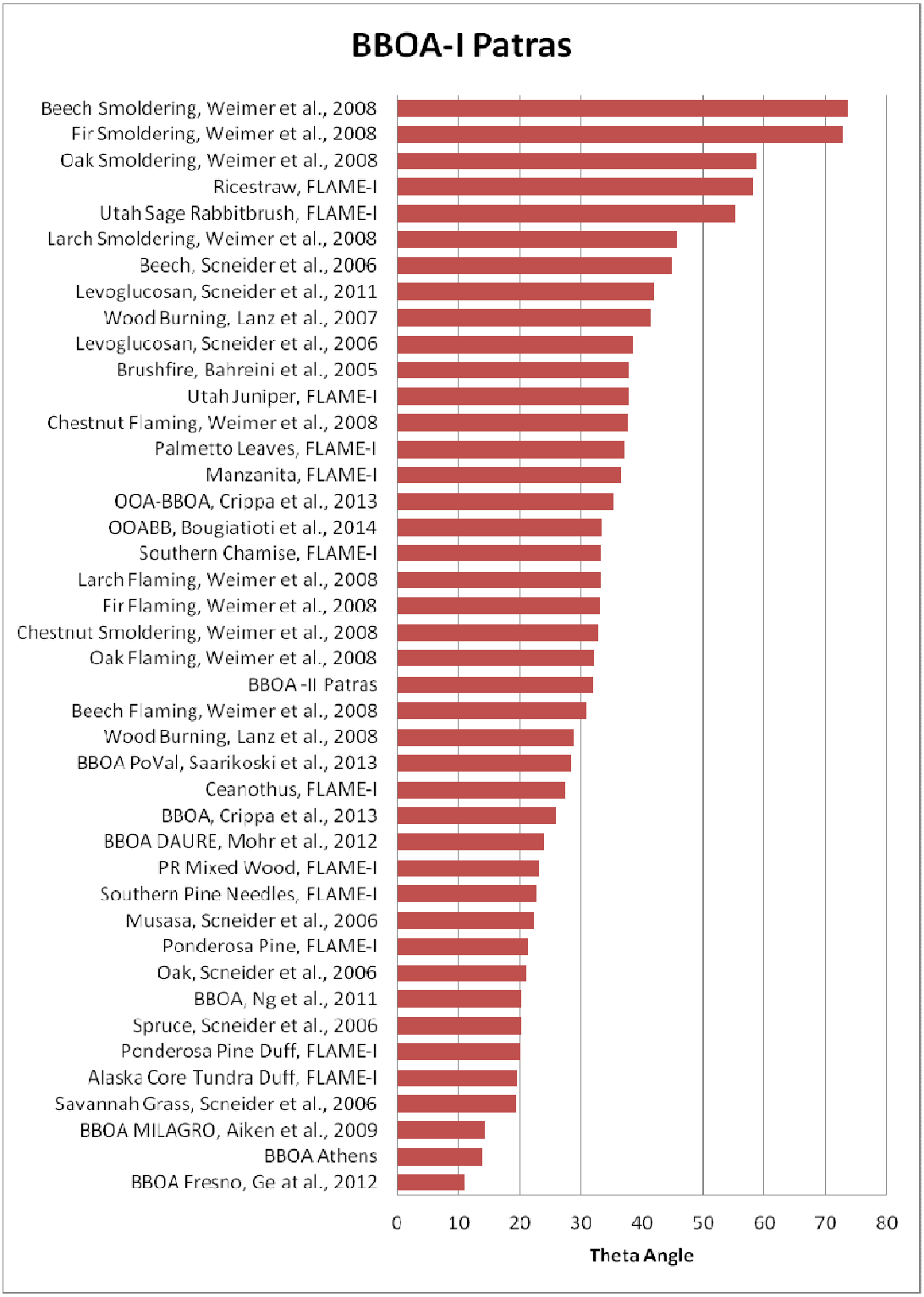


**Figure S27.** Theta angles between the BBOA-I mass spectra in Patras and BBOA from the literature.

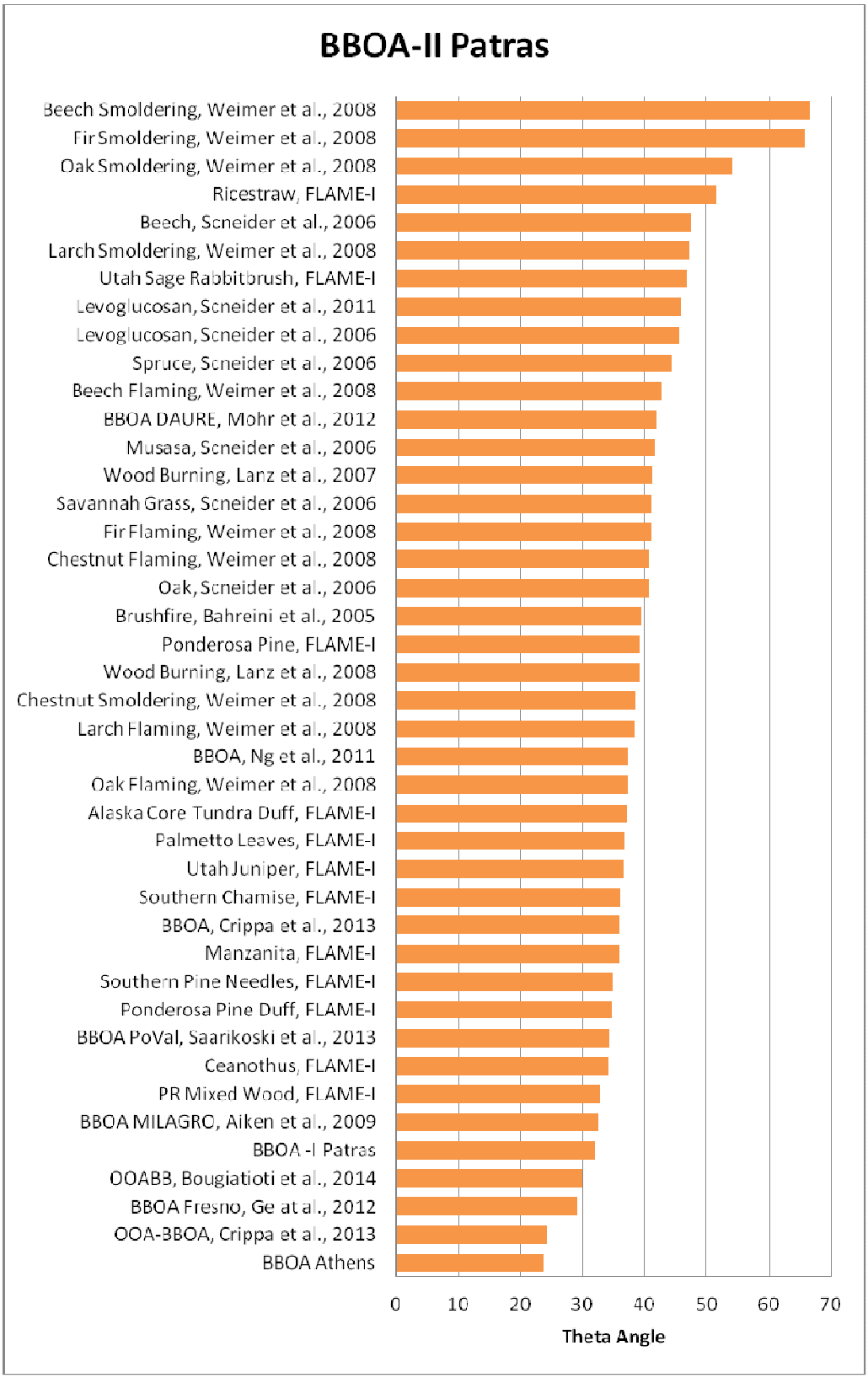


**Figure S28.** Theta angles between the BBOA-II mass spectra in Patras and BBOA from the literature.

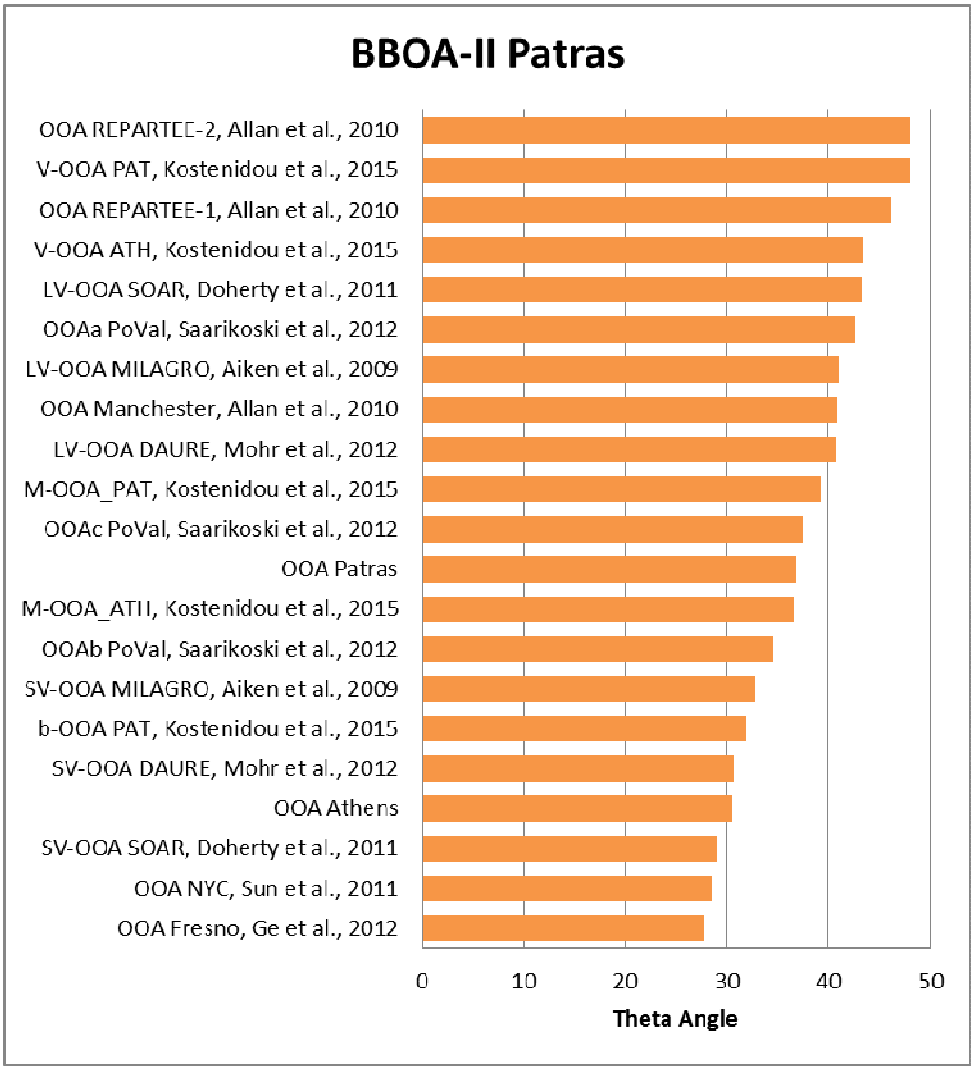


**Figure S29.** Theta angles between the BBOA-II mass spectra in Patras and OOA from the literature.

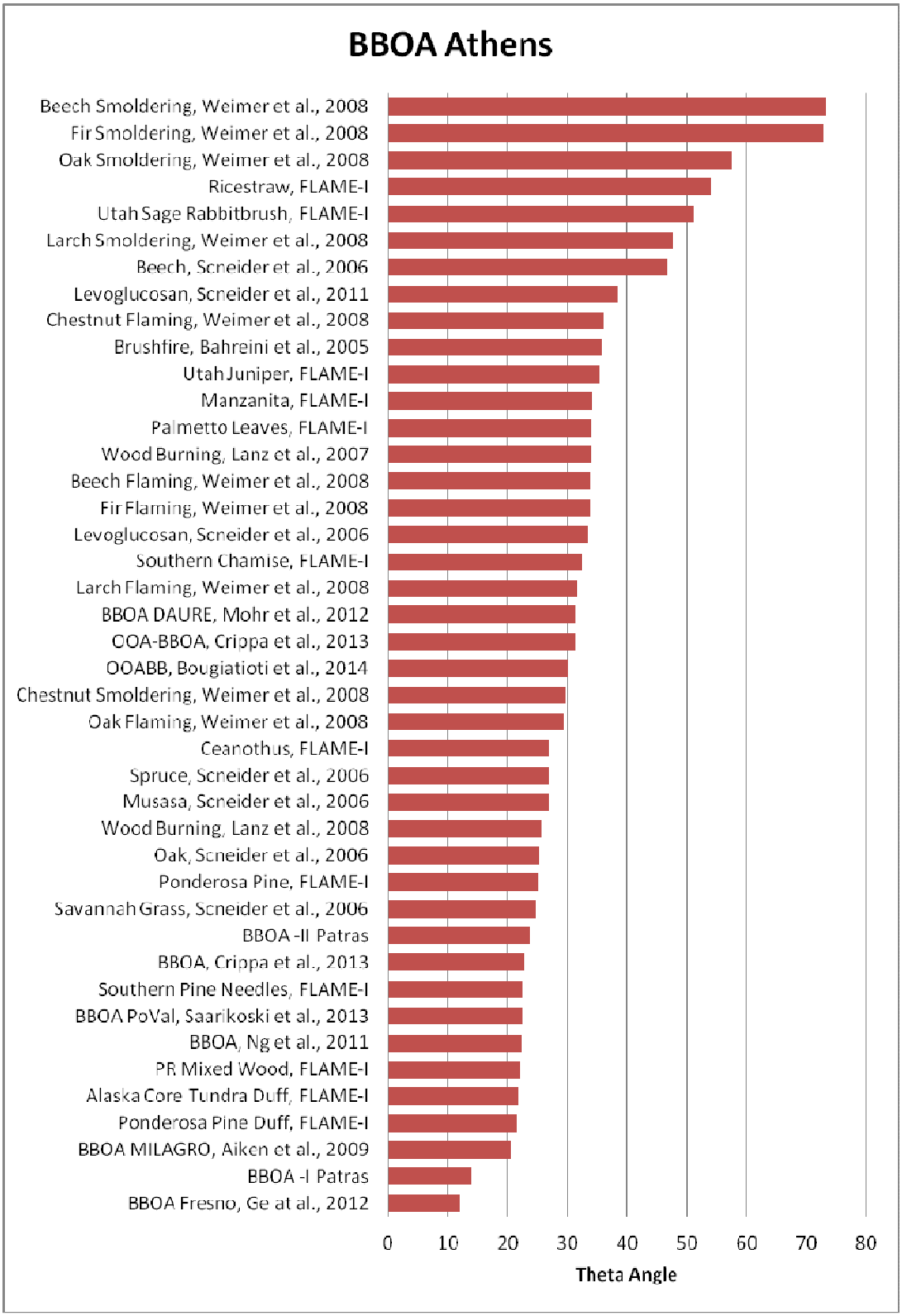


**Figure S30.** Theta angles between the BBOA mass spectra in Athens and BBOA spectra from the literature.

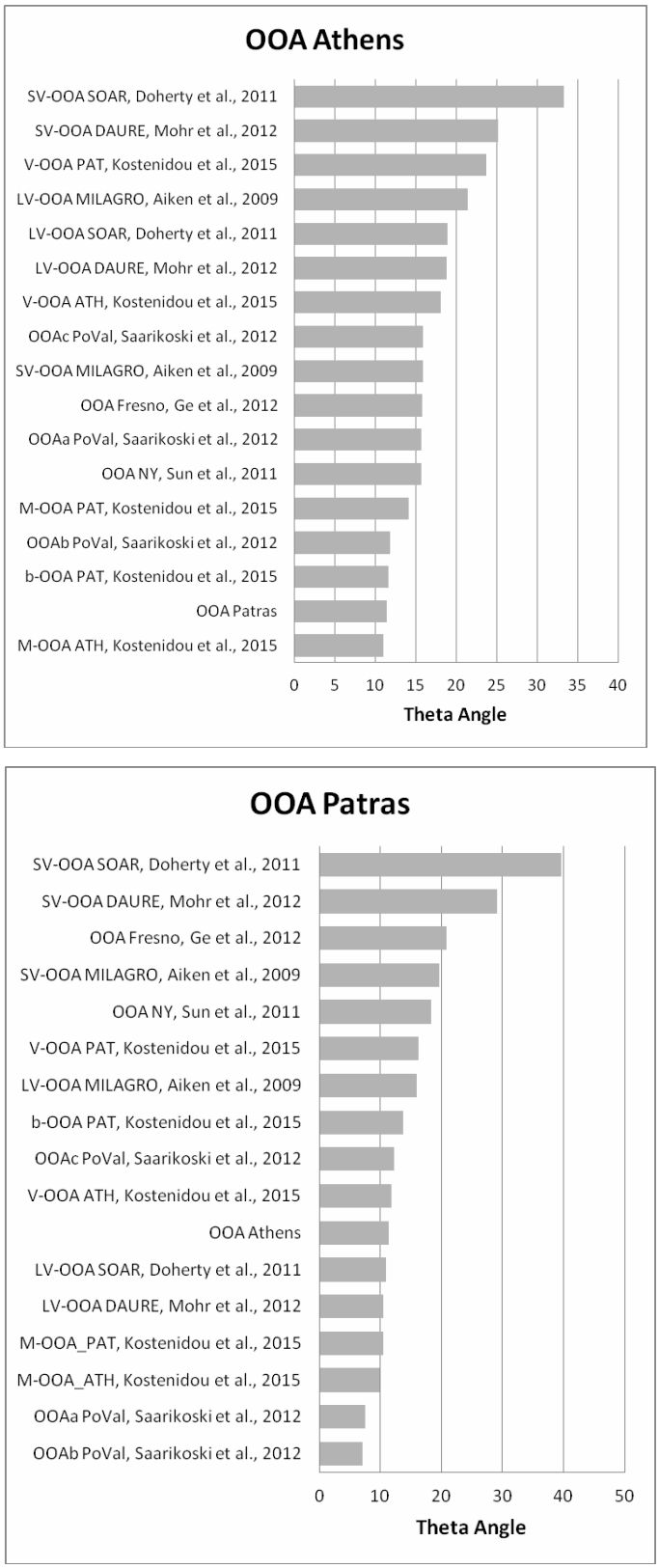


**Figure S31.** Theta angles between the OOA mass spectra in the two cities and the literature.

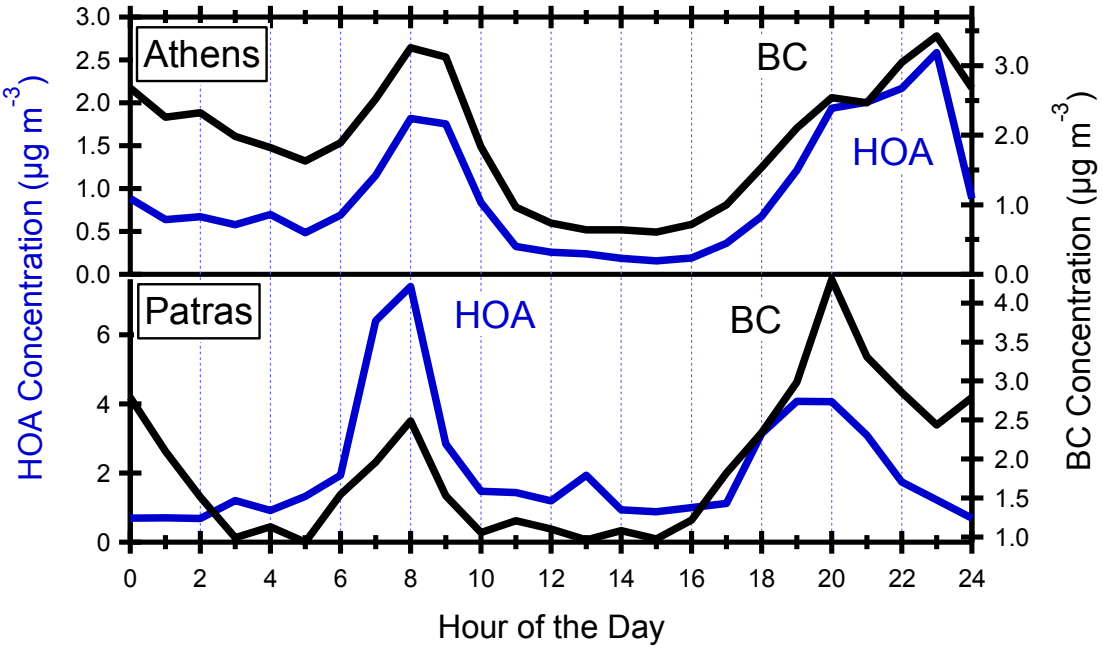


**Figure S32.** The diurnal profiles of the HOA and BC in a) Athens and b) Patras.

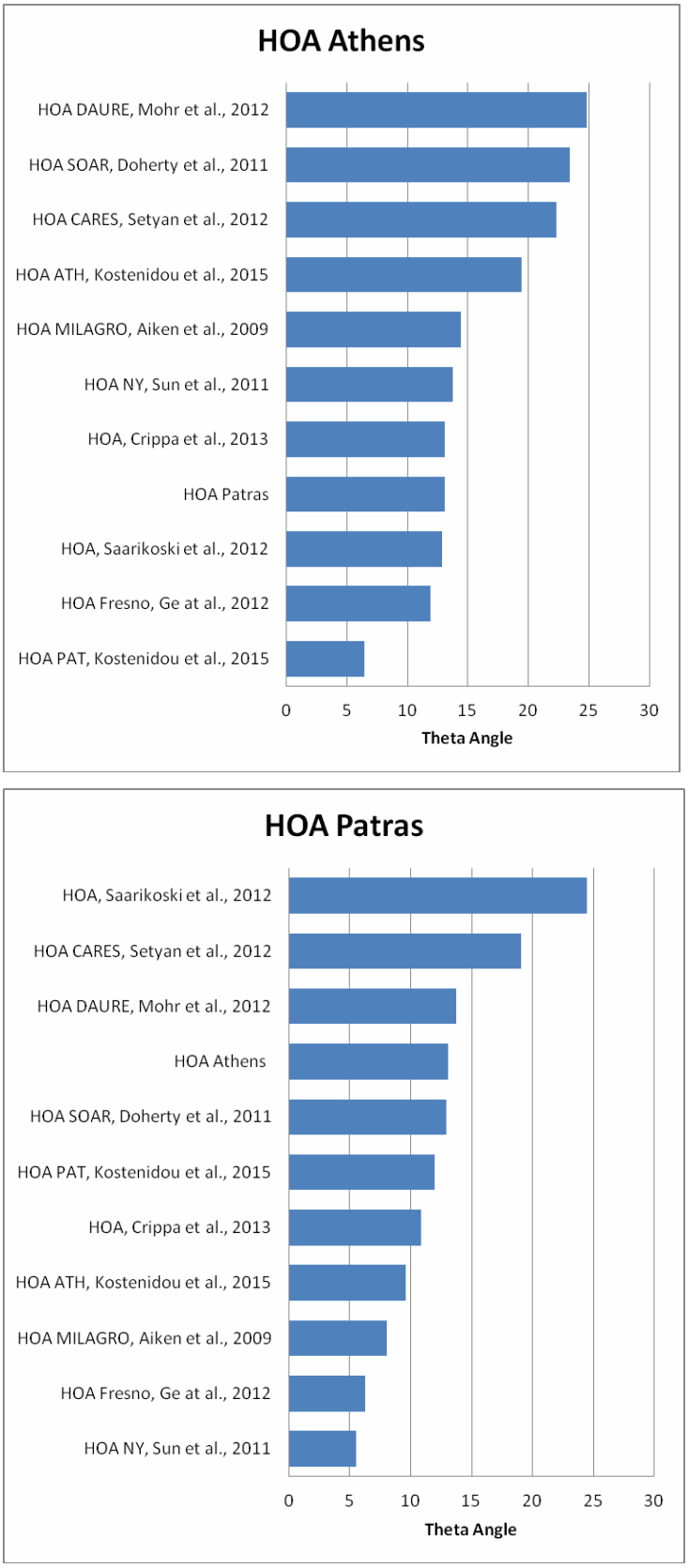


**Figure S33.** Theta angles between the HOA mass spectra in the two cities and the literature.

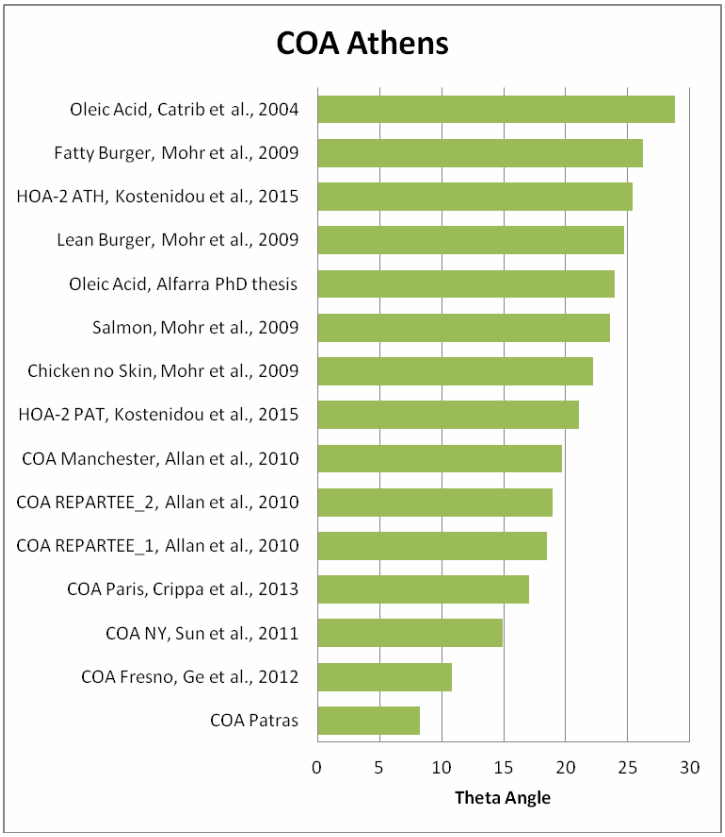


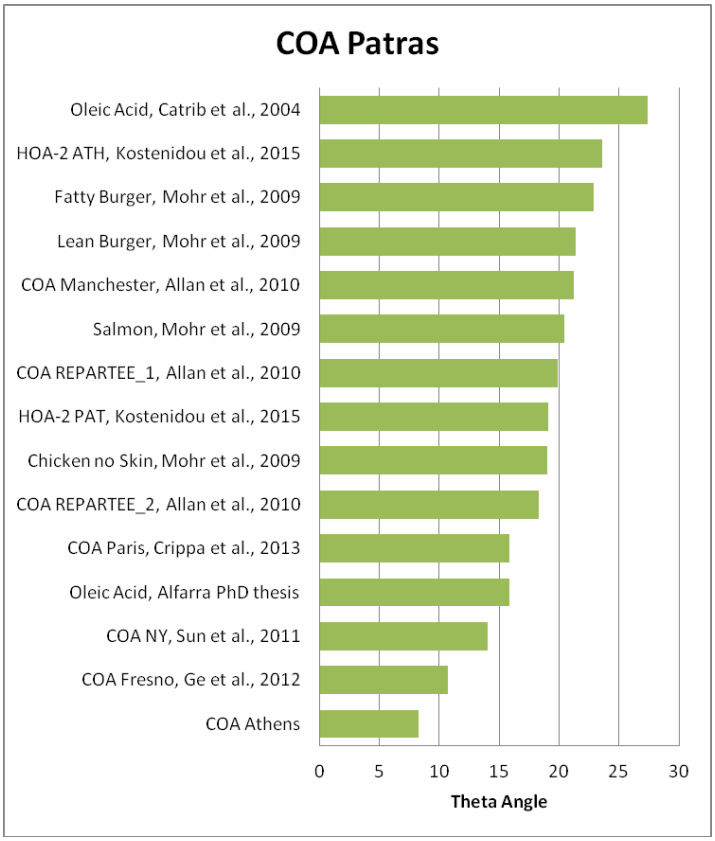


**Figure S34.** Theta angles between the COA mass spectra in the two cities and the literature.

## 10. Ng Triangles

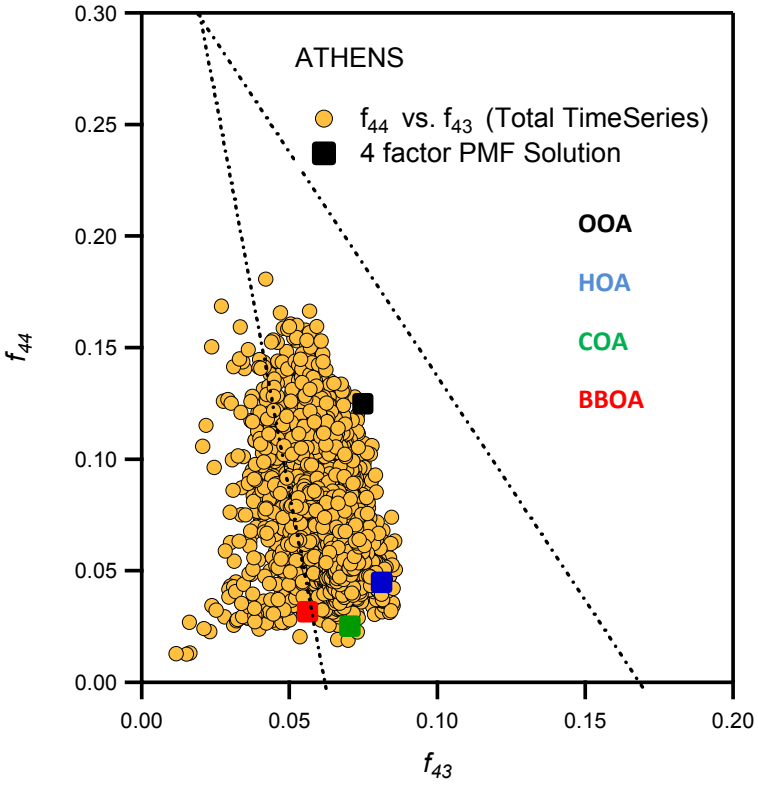


**Figure S35.** Ng triangle for the Athens campaign.

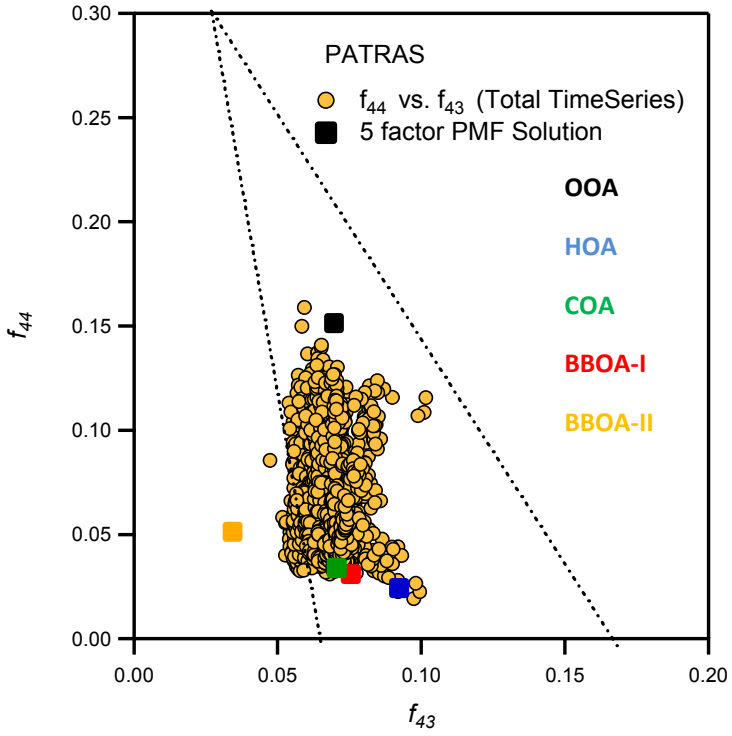


**Figure S36.** Ng triangle for the Patras campaign.